Title: Noninvasive Detection of Fetal Genetic Variations through Polymorphic Sites Sequencing of Maternal Plasma DNA

Running Title: GGAP-NIPT: a new sensitive method for NIPT

Authors: Song Gao*

Affiliations:

The State Key Laboratory Breeding Base of Basic Science of Stomatology & Key Laboratory of Oral Biomedicine Ministry of Education, School & Hospital of Stomatology, Wuhan University, Wuhan, China, 430079.

***Corresponding author**

Song Gao, School & Hospital of Stomatology, Wuhan University, 237 Luoyu Road, Wuhan, China, 430079. Email: gaos@whu.edu.cn.

Funding statement: none.

Abstract

Non-invasive prenatal testing (NIPT) for common fetal aneuploidies using circulating cell free DNA in maternal plasma has been widely adopted in clinical practice for its sensitivity and accuracy. However, the detection of subchromosomal abnormalities or monogenetic variations showed no cost-effectiveness or satisfactory accuracy. Here we describe the goodness-of-fit and graphical analysis of polymorphic sites based non-invasive prenatal testing (GGAP-NIPT) assay, which was sensitive and accurate for detecting fetal abnormalities simultaneously at the chromosomal, subchromosomal and nucleotide levels. In each sample, fetal fraction was estimated using allelic counts of polymorphic sites from normal reference chromosomal regions and each target amplicon's genotype was determined with the aid of goodness-of-fit test. Then group of polymorphic amplicons from each target region was analyzed collectively using both statistical and graphical approaches, and fetal genetic abnormality was identified by either overall statistical model fitness or graphical characteristic allelic clusters, whereas regions containing only a single polymorphic site were analyzed using a limited number of replicates. For simulated samples, such a group analytic approach identified all aneuploidies, microdeletions or microduplications and single-gene short variations precisely. As no cross-sample comparison was performed and the relative allelic counts of each target polymorphic amplicon were internally controlled, the GGAP-NIPT assay reported here should be sensitive and accurate inherently. Therefore, the GGAP-NIPT analytical approach has the potential to detect most fetal abnormalities at the chromosomal, subchromosomal and monogenic levels with improved accuracy, facilitating the extension of NIPT to an expanded panel of genetic disorders.

Keywords: NIPT, amplicon sequencing, goodness of fit, polymorphic site, GGAP, fetal fraction

Introduction

Noninvasive prenatal testing (NIPT) is now widely used for the detection of fetal chromosomal aneuploidies and certain copy number variations, where cell-free DNA (cfDNA) in maternal plasma[1] was

analyzed by whole-genome sequencing (WGS) [2,3], single-nucleotide polymorphism (SNP)[4,5] or microarray[6,7]. NIPT showed high test sensitivity and specificity for common fetal aneuploidies, such as trisomies 21, 18 and 13, but low in detecting subchromosomal deletions and duplications[8-10], especially when the genomic aberrations were small[11-15]. For monogenic disorders, different noninvasive approaches have been developed[16], but the application of such methods in clinical practice has lagged behind aneuploidy testing due to high costs and technical challenges.

In cfDNA, a certain number of polymorphic sites showed allelic imbalance due to the presence of fetal DNA and characteristic relative allelic ratios were observed when there were fetal aneuploidies. For example, when the fetus inherits a paternal allele different from the mother's (Fig. S1), fetal aneuploidies can be detected using relative allelic counts. In theory, fetal abnormalities of the maternal origin could also be detected using characteristic relative allelic distributions. Therefore, we proposed an assay, goodness-of-fit and graphical analysis of polymorphic sites based non-invasive prenatal testing (GGAP-NIPT), to detect fetal abnormalities at the chromosomal, subchromosomal and single-gene short sequence levels simultaneously, which was shown sensitive and accurate for all our simulated test samples.

Results

Fetal Fraction Estimation

To estimate fetal fraction of maternal plasma cfDNA, a panel of polymorphic markers from the sample's reference chromosomes was amplified and sequenced, followed by the counting of allelic reads for each marker. Then genotype of each marker was estimated using its allelic counts (Fig. 1a, Fig. S2) and reads counts of fetal origin were deduced (Fig. 1b, Table S1) according to the estimated marker genotype. Finally, fetal read counts were plotted against the corresponding total read counts for each marker and fetal fraction was estimated by fitting a robust linear regression model (Fig. 1c,d). A high degree of correlation was observed for fetal fractions estimated this way and that estimated using WGS method when samples from the insertion/deletion polymorphism[17] dataset were analyzed and the WGS samples

with low mapped bin counts were excluded (Fig. 1e, Fig. S3). Similarly, nearly identical fetal fraction estimates were observed for library- or sequencing-level replicates[18] (Fig. 1f), indicating that the method for fetal fraction estimation was accurate and reliable. Similar results were observed for simulated data, and the estimation accuracies for fetal fractions were affected by both the abundance of fetal materials and the sequencing coverage (Fig. S4).

Discrete Nature of Relative Allelic Counts

When both the mother and the fetus are normal diploid, one of five maternal-fetal genotypes is possible for each polymorphic site in maternal plasma DNA (Table S2). In addition, all polymorphic sites in each sample have the same overall percentage of read counts amplified from the fetal genetic materials and relative allelic counts of each genotype were only determined by the sample's fetal fraction in ideal cases. Therefore, relative allelic read counts of each polymorphic site are discrete in nature, as demonstrated by a representative sample from the replication dataset where distinct relative allelic clusters were observed for the most and second most abundant alleles (Fig 2a). Moreover, when the second most abundant relative allelic count was plotted against the most, distinct genotypic clusters were expected for each site (Fig. 2b, Table S2, Fig. S5), and such a plot could be useful for determining target site's genotype or aiding in primer design. When dealing with discrete allelic count data for each polymorphic site, goodness-of-fit test[19] was appropriate as the expected relative allelic counts could be determined for each possible genotype when the sample's fetal fraction was known or estimated (Fig. 2c), and the target genotype was estimated to be the one with the best fit statistics (Fig. 2d). Here, AIC was used for comparing non-nested genotype models for each site (Fig. 2e) and ΔAIC used for estimating the genotype fitness between different models. When analyzing the replication dataset, great ΔAIC variations were observed due to different fetal fractions and different total read counts for different polymorphic sites (Fig. S6, Fig. 2f), while nearly similar magnitude of adjusted ΔAIC values were observed (Fig. 2g), indicating that the adjusted ΔAIC could be a good measure for checking the fitness of different genotype models to

polymorphic sites with different sequencing depths. As expected, more than 95% of the maternal-fetal genotypes could be correctly estimated for polymorphic sites of simulated cfDNA samples when the sequencing coverage was ≥2000 and the fetal fraction was ≥0.05 (Fig. S7).

Detection of Chromosomal Aneuploidies

When there was a fetal aneuploidy, all polymorphic sites on the target chromosome were affected, and the relative allelic counts for each polymorphic site should be changed due to the absence of one chromosome or the presence of one extra chromosome (Table S2-S4). To detect chromosomal aneuploidy, a panel of polymorphic sites on the target chromosome was amplified and allelic read counts for each site were calculated. Then two genotypes were estimated for each site, whereas one assuming that the fetal chromosome was normal and another one assuming that the fetal chromosome was aneuploidy. Finally, polymorphic sites on the target chromosome were analyzed collectively, and the overall fitness of all sites to the normal chromosome model was compared with that of the aneuploidy model (Fig. 3a). Such an approach might seem unsound mathematically, but were sensitive and reliable to detect chromosomal aneuploidies for our simulated samples, possibly due to its similarity to repeated tests of goodness-of-fit[19] where each polymorphic site was considered as an experimental repetition. As the majority of target polymorphic sites were informative for estimating fetal aneuploidies (Fig. 3c,e) except for one-allele sites, all normal and aneuploidy chromosomes were correctly identified (Fig. S8, Fig. 3b,d) when samples with both low sequencing coverage and low fetal fraction were excluded. As expected (Fig. 3f,g), distinct clusters were observed when the second or fourth most abundant relative allelic count was plotted against the most abundant for each polymorphic site and such characteristic cluster distribution was informative enough to identify fetal aneuploidies (Fig. 3h-i, Fig. S9-S10). When estimating the genotype of a polymorphic amplicon using allelic goodness-of-fit test, it is essential that the true model is included in the analysis, as one genotype model would be selected anyway based on relative comparisons even if none of the tested models was appropriate for the data. Therefore, all possible maternal-fetal aneuploidy models for the target chromosome should be checked. For example, when detecting sex chromosome

aneuploidies, both the normal (XX and XY) and all five of the better-known sex aneuploidies (XO, XXY, XXX, XYY and XXYY)[20] should be considered.

Detecting Subchromosomal Abnormalities

To detect subchromosomal abnormalities, abnormal models for either the mother, the fetus or both should be considered if necessary, as the heterozygotes for some subchromosomal microdeletions[21] or microduplications[22] could be phenotypically normal. Based on statistics, some subchromosomal regions could be tested using models assuming that the mother was homozygous normal, while some other regions should be tested using all possible models assuming that the mother was either heterozygous or homozygous for the target abnormality (Fig. 4a). As expected, subchromosomal microdeletions or microduplications could be detected with accuracy when at least two alleles were detected for some polymorphic sites in the target region (Fig. 4b-g). When only one allele was observed for all sites in the subchromosomal region, alternative noninvasive or invasive approaches should be performed, as the allelic count approach reported here could not distinguish the monosomy-nullisomy model from the nullisomy-monosomy model due to the lack of genetic polymorphism (Table S5). When best overall fits to both a disomy-disomy model and a tetrasomy-tetrasomy model were observed for a microduplication, the target was estimated to be disomy-disomy, as each genotype in the disomy-disomy model had a corresponding counterpart in the tetrasomy-tetrasomy model with identical relative allelic distributions (for example, AB|AA corresponds to AABB|AAAA). However, not all genotypes in the tetrasomy-tetrasomy model had counterparts in the disomy-disomy model, therefore the tetrasomy-tetrasomy model should show overall best fit for all polymorphic sites but not for the disomy-disomy model if the subchromosomal region was a tetrasomy-tetrasomy homozygous-homozygous microduplication (Fig. S12). In addition, distinct clusters were observed when the second or third most abundant relative allelic count was plotted against the most abundant for each polymorphic site in the subchromosomal region and such characteristic cluster distribution was informative enough to determine fetal subchromosomal abnormalities (Fig. 4h-k, Table S5-S6, Fig. S11-S12). When allelic clusters were not in the expected

positions, either the true model was excluded and wrong model was fitted or there were non-random outliers. In such a case, further analyses, optimizing test routines or checking additional models should be followed.

Detection of Short Genetic Variations

Single-base-pair substitutions, small (≤20bp) deletions, small (≤20bp) insertions and small (≤20bp) indels are the major types of mutations associated with human inherited diseases reported in the Human Gene Mutation Database (HGMD)[23]. To detect such genetic variations in cfDNA samples, each target site was amplified and its genotype estimated using allelic goodness-of-fit test (Fig. 5a). Then the nucleotide sequence of each target allele was compared with the wildtype sequence, and fetal disease status was determined accordingly (Fig. 5a,c). As genotype estimation using a single target site was not perfect, library or sequencing level repeats were desired (Fig. S13). On the other hand, sequencing with replicates increased the overall cost considerably, and it was not cost effective when used for detecting genetic mutations with low disease prevalence. Therefore, a limited number of replicates were suggested initially for each target site with low disease prevalence, and if mutant alleles were detected for a target site, further analysis and possibly retesting using more replicates were performed. Such a two-tier test strategy could reduce the overall cost greatly and increase the positive predictive value (PPV), as only a small number of target sites were to be retested and disease incidences were increased for retested targets. Graphically, when the mutant relative allelic counts of each site were plotted against the wildtype, distinct clusters were observed for different maternal-fetal genotypes (Fig. 5b, Table S7, S8), and such a plot was sensitive enough to detect fetal short genetic variations (Fig. 5d,e).

Discussion

Currently, cfDNA based NIPT approaches have been widely available for detecting fetal aneuploidies[2-5], subchromosomal abnormalities[12,15] or monogenic diseases[24-30] in clinical practice. However, no approach

reported so far could detect genetic variations simultaneously at both the chromosomal/subchromosomal level and the nucleotide level. Here we reported a method enabling the detection of genetic abnormalities simultaneously at different genetic levels through amplicon sequencing of specific polymorphic targets. Although different sensitivities were reported when detecting genetic abnormalities at different levels[31], the sensitivity for our reported approach should not varied much, as all relative allelic information were encoded in amplified amplicons for each polymorphic site and different alleles of each amplicon had nearly identical sequences with similar amplification properties. In clinical settings, accuracy, specificity and sensitivity should be addressed using real cfDNA samples, as clinical data was inherently noisy and discrepancies between the genotypes of maternal plasma fetal DNA and the fetal genomes were reported in some samples possibly due to confined placental mosaicism[32]. For our reported method, prior knowledge about the detecting targets was required and no off-target variations could be detected[33], while WGS-based NIPT methods could detect incidental variations with no additional cost.

To detect chromosomal, subchromosomal and sequence-level abnormalities, our method required the amplification of a panel of polymorphic sites from normal reference chromosomes for estimating the sample's fetal fraction, a panel of polymorphic sites on the target chromosomal/subchromosomal regions for detecting long length abnormalities, and specific target sites possibly with replications for short length mutations. If it is challenging for amplifying all targets in a single tube, independent amplifications using multiple tubes could be performed and such an approach would not affect the analyzing results, as each amplicon could be considered as an independent data point and no cross-sample or cross-amplicon comparisons were performed. As nearly all amplification products were used for the identification of target genetic abnormalities, it should be cost-effective, while the WGS-based approaches used only a fraction of reads mapped to the target chromosomes for abnormality detection.

In principle, target amplicon sequencing could be applied to detect other genetic variations as well. For examples, chromosomal inversion or translocation with known break point could be detected by amplicons covering the specific breakpoint. Genomic abnormalities for preimplantation embryos or non-

pregnant samples could also be detected using assays similar to the reported approach, as distinct allelic distributions for all target polymorphic sites were informative enough to identify different abnormalities (Fig. S14). For cfDNA sample from a surrogate mother, fetal fraction was first estimated and updated iteratively using relative allelic counts of polymorphic sites and allelic goodness-of-fit test (Fig. S15), then genetic variations could be detected by checking all possible genotype models. For samples from a mother with multiple pregnancies, fetal fraction for each fetus could be estimated using a similar approach (Fig. S15), where each fetal fraction estimate was updated iteratively until converge, and genetic abnormalities could be detected using allelic goodness-of-fit test, whereas expected allelic counts for each polymorphic site could be calculated when fetal fractions for all fetuses were available.

Collectively, nearly all common genetic disorders could be detected with the aid of polymorphic amplicon sequencing, and expansion of NIPT to detect both genetic conditions that were common to all pregnancies and disorders that had high prevalence in particular groups would have great socioeconomic benefits.

Materials and Methods

Dataset

The insertion/deletion polymorphism[17] dataset (BioProject ID: PRJNA387652) and the replication[18] dataset (BioProject ID: PRJNA517742) were retrieved from the NCBI SRA database. The simulated datasets were generated using ART[34] simulator (Supplementary Information for detailed descriptions).

Reads Processing and Mapping

Reads retrieved from SRA or simulated were filtered out using custom scripts where the low quality bases were removed and the longest subsequence in each read was retained so that all bases had a quality score greater than 14. Whole genome sequencing reads were mapped by bowtie2[35]. For amplicon reads, one or

several unique 12-mer indexes were extracted from each amplicon and each read was mapped to an amplicon using such indexes. Then the allelic reads for each amplicon in each sample were counted using unique allelic sequences.

Fetal Fraction Estimation by Allelic Read Counts

For amplicon sequencing data, fetal fractions were estimated as follows. For each polymorphic site, read counts for all alleles were sorted in descending order and labeled as R1, R2, R3, etc. Then the possible maternal-fetal genotype was estimated using allelic read counts (Fig. S2) followed by the estimation of fetal and total read counts (Table S1). Finally, fetal fraction was estimated using fetal and total read counts and a robust linear regression model (Supplementary Methods).

Fetal Fraction Estimation by Whole Genome Sequencing

Fetal fraction was calculated as described using the formula[36]

Fetal Fraction $(f)=\frac{2.0\times \mathrm{med}(\mathrm{Chr_Y})}{\mathrm{med}(\mathrm{Chr_X})+\mathrm{med}(\mathrm{Chr_Y})}$, where $\mathrm{med}(\mathrm{Chr_X})$ and $\mathrm{med}(\mathrm{Chr_Y})$ represent the median read counts of the 50-kb bins on the X and Y chromosomes, respectively. Briefly, the 50-kb bins from the X and Y chromosomes were extracted and bins having too low or too high read counts were filtered out using 200 whole genome sequencing samples (SRR6040419-SRR6040618) from the project PRJNA400134[37] as follows. Reads were firstly mapped to the human reference genome using bowtie2[35], and total reads mapped into each X or Y bin were counted for each sample using custom scripts. Subsequently, X bins containing no mapped reads in more than 25% of the samples or containing read counts not in the range of Median±3.0×MAD_e were removed, while Y bins containing at least one read in more than 25% of the female pregnancies, containing no mapped reads in more than 25% of the male pregnancies or containing read counts not in the range of Median±3.0×MAD_e were removed as well. Hence, a total of 2760 chromosome X bins and 192 chromosome Y bins were identified as informative

bins. Fetal fractions for the 61 samples from PRJNA387652 were calculated using the median count values of X bins and Y bins as described above.

Maternal-Fetal Genotype Estimation

Fetal fraction was estimated first for each sample. Then for each polymorphic site, reads for each allele were counted, followed by the calculations of AICs for all possible genotype models using goodness-of-fit test. Finally, the genotype for each polymorphic site was estimated to be the one with the minimal AIC, and ΔAIC was calculated as the absolute difference between the minimal AIC and the second minimal AIC. To detect chromosomal or subchromosomal genotypes, the minimal AICs for all allelic sites was averaged for each chromosomal/subchromosomal model, and the chromosomal/subchromosomal genotype was estimated to be the one associated with the minimal average AIC (Supplementary Methods).

Statistical Analysis

Statistical analysis was performed in R[38] (version 3.5.1). AICs were calculated using custom scripts.

Acknowledgements

The author would like to thank Yongxin Ke for technical and administrative assistance, discussions and comments on the project, and Min Nie for her comments, insightful suggestions and careful editing of the manuscript.

Author Contributions

S. G. designed the experiments, performed the experiments, analyzed the data and wrote the manuscript.

Conflict of Interest

A patent application has been filed relating to this project.

References

1 Lo, Y. M. *et al.* Presence of fetal DNA in maternal plasma and serum. *Lancet* **350**, 485-487, doi:10.1016/s0140-6736(97)02174-0 (1997).

2 Fan, H. C., Blumenfeld, Y. J., Chitkara, U., Hudgins, L. & Quake, S. R. Noninvasive diagnosis of fetal aneuploidy by shotgun sequencing DNA from maternal blood. *Proceedings of the National Academy of Sciences of the United States of America* **105**, 16266-16271, doi:10.1073/pnas.0808319105 (2008).

3 Chiu, R. W. *et al.* Noninvasive prenatal diagnosis of fetal chromosomal aneuploidy by massively parallel genomic sequencing of DNA in maternal plasma. *Proceedings of the National Academy of Sciences of the United States of America* **105**, 20458-20463, doi:10.1073/pnas.0810641105 (2008).

4 Zimmermann, B. *et al.* Noninvasive prenatal aneuploidy testing of chromosomes 13, 18, 21, X, and Y, using targeted sequencing of polymorphic loci. *Prenat Diagn* **32**, 1233-1241, doi:10.1002/pd.3993 (2012).

5 Liao, G. J. *et al.* Noninvasive prenatal diagnosis of fetal trisomy 21 by allelic ratio analysis using targeted massively parallel sequencing of maternal plasma DNA. *PLoS One* **7**, e38154, doi:10.1371/journal.pone.0038154 (2012).

6 Srebniak, M. I. *et al.* The influence of SNP-based chromosomal microarray and NIPT on the diagnostic yield in 10,000 fetuses with and without fetal ultrasound anomalies. *Hum Mutat* **38**, 880-888, doi:10.1002/humu.23232 (2017).

7 Juneau, K. *et al.* Microarray-based cell-free DNA analysis improves noninvasive prenatal testing. *Fetal Diagn Ther* **36**, 282-286, doi:10.1159/000367626 (2014).

8 Hu, H. *et al.* Noninvasive prenatal testing for chromosome aneuploidies and subchromosomal microdeletions/microduplications in a cohort of 8141 single pregnancies. *Human Genomics* **13**, 14, doi:10.1186/s40246-019-0198-2 (2019).

9 Srebniak, M. I. *et al.* Social and medical need for whole genome high resolution NIPT. *Mol Genet Genomic Med* **8**, e1062, doi:10.1002/mgg3.1062 (2020).

10 Advani, H. V., Barrett, A. N., Evans, M. I. & Choolani, M. Challenges in non-invasive prenatal screening for sub-chromosomal copy number variations using cell-free DNA. *Prenat Diagn* **37**, 1067-1075, doi:10.1002/pd.5161 (2017).

11 Chau, M. H. K. *et al.* Characteristics and mode of inheritance of pathogenic copy number variants in prenatal diagnosis. *Am J Obstet Gynecol*, doi:10.1016/j.ajog.2019.06.007 (2019).

12 Lo, K. K. *et al.* Limited Clinical Utility of Non-invasive Prenatal Testing for Subchromosomal Abnormalities. *Am J Hum Genet* **98**, 34-44, doi:10.1016/j.ajhg.2015.11.016 (2016).

13 Yu, S. C. *et al.* Noninvasive prenatal molecular karyotyping from maternal plasma. *PLoS One* **8**, e60968, doi:10.1371/journal.pone.0060968 (2013).

14 Li, R. *et al.* Detection of fetal copy number variants by non-invasive prenatal testing for common aneuploidies. *Ultrasound Obstet Gynecol* **47**, 53-57, doi:10.1002/uog.14911 (2016).

15 Yin, A. H. *et al.* Noninvasive detection of fetal subchromosomal abnormalities by semiconductor sequencing of maternal plasma DNA. *Proceedings of the National Academy of Sciences of the United States of America* **112**, 14670-14675, doi:10.1073/pnas.1518151112 (2015).

16 Allen, S., Young, E. & Gerrish, A. in *Noninvasive Prenatal Testing (NIPT)* (eds Lieve Page-Christiaens & Hanns-Georg Klein) 157-177 (Academic Press, 2018).

17 Barrett, A. N. *et al.* Measurement of fetal fraction in cell-free DNA from maternal plasma using a panel of insertion/deletion polymorphisms. *PLoS One* **12**, e0186771, doi:10.1371/journal.pone.0186771 (2017).

18 Kim, J. *et al.* The use of technical replication for detection of low-level somatic mutations in next-generation sequencing. *Nat Commun* **10**, 1047, doi:10.1038/s41467-019-09026-y (2019).

19 McDonald, J. H. *Handbook of Biological Statistics*. Third edn, (Sparky House Publishing, Baltimore, Maryland, 2014).

20 Skuse, D., Printzlau, F. & Wolstencroft, J. Sex chromosome aneuploidies. *Handb Clin Neurol* **147**, 355-376, doi:10.1016/b978-0-444-63233-3.00024-5 (2018).

21 Milili, M. *et al.* A new case of autosomal recessive agammaglobulinaemia with impaired pre-B cell differentiation due to a large deletion of the IGH locus. *European Journal of Pediatrics* **161**, 479-484, doi:10.1007/s00431-002-0994-9 (2002).

22 Ceylan, A. C. *et al.* Autosomal recessive spinocerebellar ataxia 18 caused by homozygous exon 14 duplication in GRID2 and review of the literature. *Acta Neurol Belg*, doi:10.1007/s13760-020-01328-z (2020).

23 Stenson, P. D. *et al.* The Human Gene Mutation Database (HGMD) and its exploitation in the fields of personalized genomics and molecular evolution. *Curr Protoc Bioinformatics* **Chapter 1**, Unit1 13, doi:10.1002/0471250953.bi0113s39 (2012).

24 Yin, X. *et al.* Identification of a de novo fetal variant in osteogenesis imperfecta by targeted sequencing-based noninvasive prenatal testing. *J Hum Genet* **63**, 1129-1137, doi:10.1038/s10038-018-0489-9 (2018).

25 Zhang, J. *et al.* Non-invasive prenatal sequencing for multiple Mendelian monogenic disorders using circulating cell-free fetal DNA. *Nat Med* **25**, 439-447, doi:10.1038/s41591-018-0334-x (2019).

26 Lv, W. *et al.* Noninvasive Prenatal Testing for Wilson Disease by Use of Circulating Single-Molecule Amplification and Resequencing Technology (cSMART). *Clinical Chemistry* **61**, 172-181, doi:10.1373/clinchem.2014.229328 (2015).

27 Cutts, A. *et al.* A method for noninvasive prenatal diagnosis of monogenic autosomal recessive disorders. *Blood* **134**, 1190-1193, doi:10.1182/blood.2019002099 (2019).

28 Lun, F. M. *et al.* Noninvasive prenatal diagnosis of monogenic diseases by digital size selection and relative mutation dosage on DNA in maternal plasma. *Proceedings of the National Academy of Sciences of the United States of America* **105**, 19920-19925, doi:10.1073/pnas.0810373105 (2008).

29 Lo, Y. M. *et al.* Maternal plasma DNA sequencing reveals the genome-wide genetic and mutational profile of the fetus. *Sci Transl Med* **2**, 61ra91, doi:10.1126/scitranslmed.3001720 (2010).

30 Vermeulen, C. *et al.* Sensitive Monogenic Noninvasive Prenatal Diagnosis by Targeted Haplotyping. *Am J Hum Genet* **101**, 326-339, doi:10.1016/j.ajhg.2017.07.012 (2017).

31 Suciu, I. D., Toader, O. D., Galeva, S. & Pop, L. Non-Invasive Prenatal Testing beyond Trisomies. *Journal of medicine and life* **12**, 221-224, doi:10.25122/jml-2019-0053 (2019).

32 Brady, P. *et al.* Clinical implementation of NIPT - technical and biological challenges. *Clin Genet* **89**, 523-530, doi:10.1111/cge.12598 (2016).

33 Renga, B. Non invasive prenatal diagnosis of fetal aneuploidy using cell free fetal DNA. *Eur J Obstet Gynecol Reprod Biol* **225**, 5-8, doi:10.1016/j.ejogrb.2018.03.033 (2018).

34 Huang, W., Li, L., Myers, J. R. & Marth, G. T. ART: a next-generation sequencing read simulator. *Bioinformatics* **28**, 593-594, doi:10.1093/bioinformatics/btr708 (2012).

35 Langmead, B. & Salzberg, S. L. Fast gapped-read alignment with Bowtie 2. *Nat Methods* **9**, 357-359, doi:10.1038/nmeth.1923 (2012).

36 van Beek, D. M. *et al.* Comparing methods for fetal fraction determination and quality control of NIPT samples. *Prenat Diagn* **37**, 769-773, doi:10.1002/pd.5079 (2017).

37 Xu, H. *et al.* Informative priors on fetal fraction increase power of the noninvasive prenatal screen. *Genet Med* **20**, 817-824, doi:10.1038/gim.2017.186 (2018).

38 R Core Team. R: A Language and Environment for Statistical Computing. (2020).

Figures:

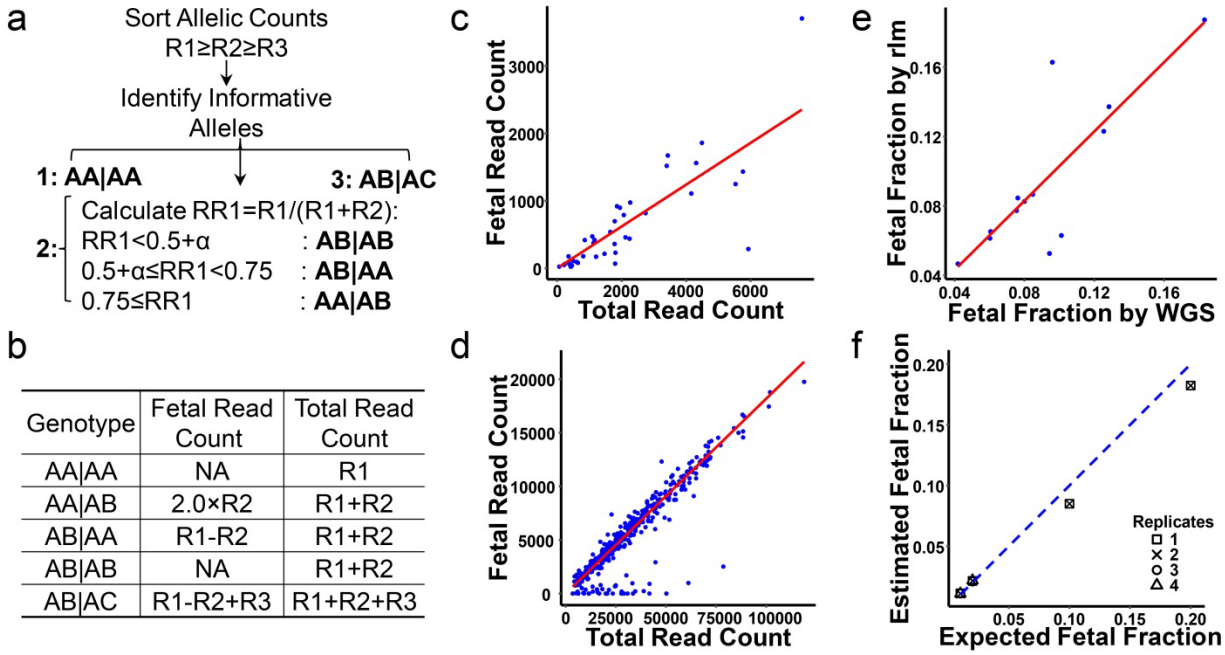

Genotype	Fetal Read Count	Total Read Count
AA|AA	NA	R1
AA|AB	2.0×R2	R1+R2
AB|AA	R1-R2	R1+R2
AB|AB	NA	R1+R2
AB|AC	R1-R2+R3	R1+R2+R3

Fig. 1:Fetal fraction estimation. a, Genotype estimation for each polymorphic site using allelic counts. **b**, Expected fetal read count and total read count for each genotype. **c, d,** Representative plots from the insertion/deletion polymorphism dataset (**c**) and replication dataset (**d**). A robust linear regression line was fitted (red line, model y=βx+0), and fetal fraction was estimated to be the model coefficient (β). **e**, Fetal fractions were estimated for each insertion/deletion polymorphism sample by both allelic read counts method (rlm) and WGS method (red line was the fitted regression line y~x), excluding WGS samples with low bin counts for chromosome X (<100) or Y (<4). **f**, Expected and estimated fetal fractions for replication samples (blue line: y=x). α: background noise threshold.

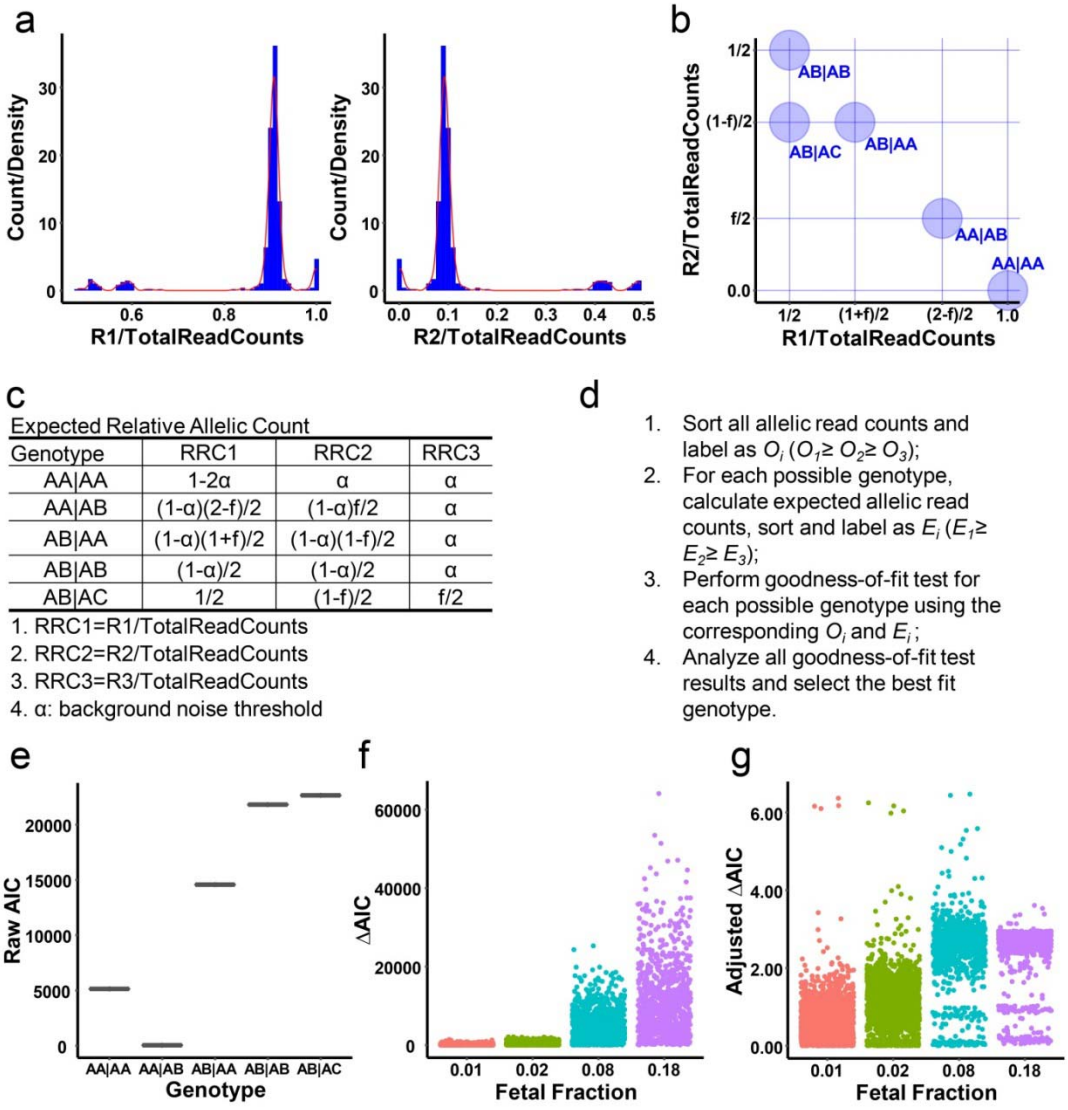

Fig. 2: Maternal-fetal genotype estimation. a, Discrete clusters of relative allelic counts for a representative sample from the replication dataset (blue: histogram count, red: density). **b**, Expected relative allelic clusters for polymorphic sites on normal reference chromosomes. **c**, Expected relative allelic counts for each normal maternal-fetal genotype. **d**, Steps to estimate maternal-fetal genotype for each polymorphic site (allelic goodness-of-fit test). **e**, A representative plot for genotype estimation using allelic goodness-of-fit test. **f, g**, ΔAIC (**f**) and adjusted ΔAIC (**g**) were calculated for each polymorphic site of the replicate samples grouped by estimated fetal fraction. ΔAIC= the second minimal AIC- the minimal AIC. Adjusted ΔAIC= ΔAIC/TotalCount/FetalFraction.

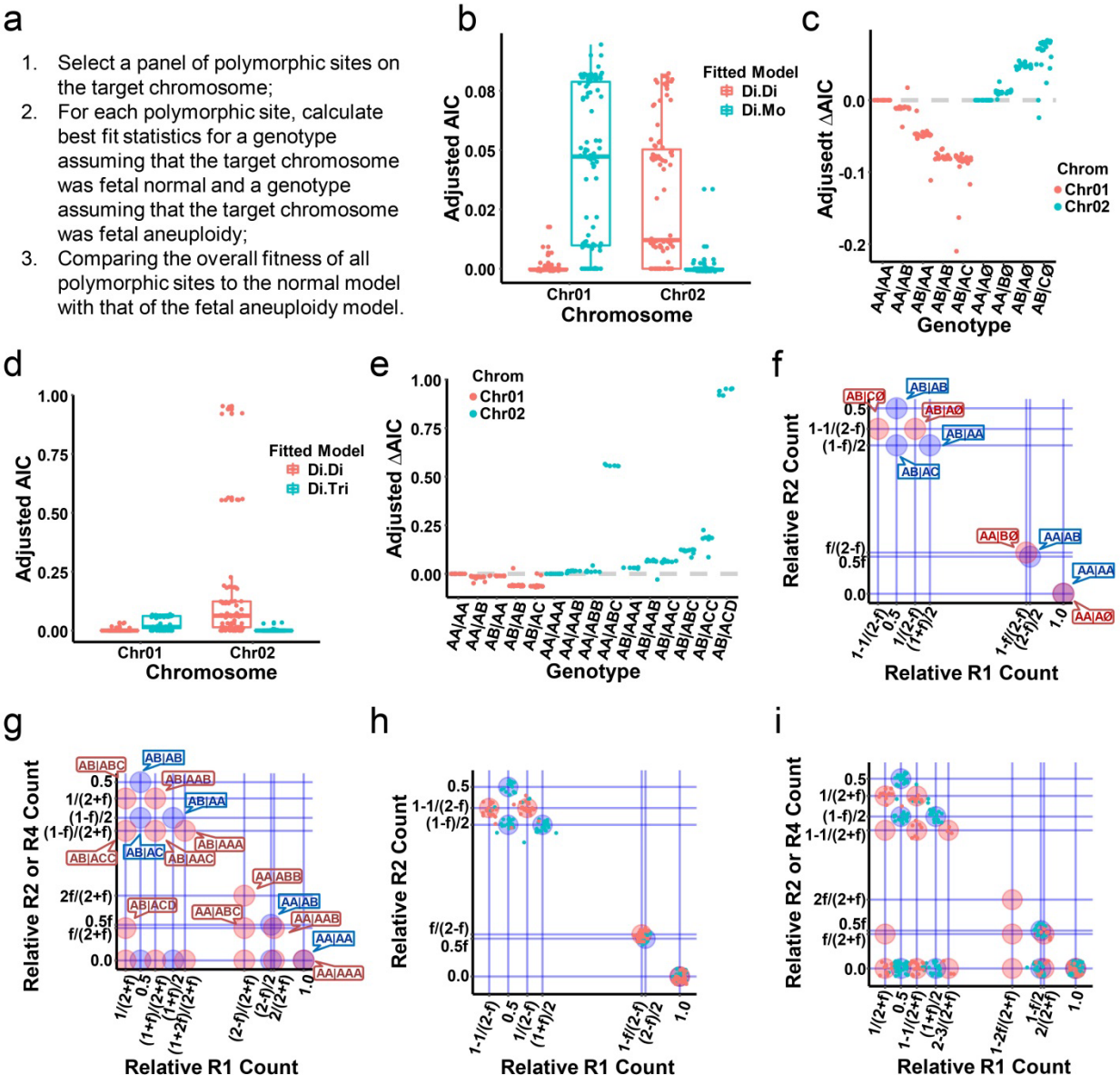

Fig. 3: Fetal aneuploidy detection. a, Steps to detect fetal aneuploidy using overall goodness-of-fit test for all polymorphic sites. **b**, A representative plot for overall goodness-of-fit tests of two simulated chromosomes. Chr01, simulated disomy-disomy chromosome (Di.Di); Chr02, simulated disomy-monosomy chromosome (Di.Mo). **c**, Contributions of different genotypes to the detection of fetal monosomy for two simulated chromosomes (Chr01, Di.Di; Chr02, Di.Mo). Adjusted ΔAIC= the minimal adjusted AIC for Di.Di model - the minimal adjusted AIC for Di.Mo model. **d,** A representative plot for overall goodness-of-fit tests of two simulated chromosomes. Chr01, Di.Di; Chr02, simulated disomy-

trisomy chromosome (Di.Tri). **e**, Contributions of different genotypes to the detection of fetal trisomy for two simulated chromosomes (Chr01, Di.Di; Chr02, Di.Tri). Adjusted ΔAIC= the minimal adjusted AIC for Di.Di model - the minimal adjusted AIC for Di.Tri model. **f, g,** Expected relative allelic clusters of polymorphic sites for fetal monosomy (**f**) or fetal trisomy (**g**) detection. **h,** Detection of fetal monosomy. Relative allelic counts for polymorphic sites on the reference chromosome (blue) and the target chromosome (red) were plotted for a representative sample. From the characteristic cluster positions, the target chromosome was estimated to be normal for the mother but monosomy for the fetus. **i**, Detection of fetal trisomy. Relative allelic counts for polymorphic sites on the reference chromosome (blue) and the target chromosome (red) were plotted for a representative sample. From the characteristic cluster positions, the target chromosome was estimated to be normal for the mother but trisomy for the fetus.

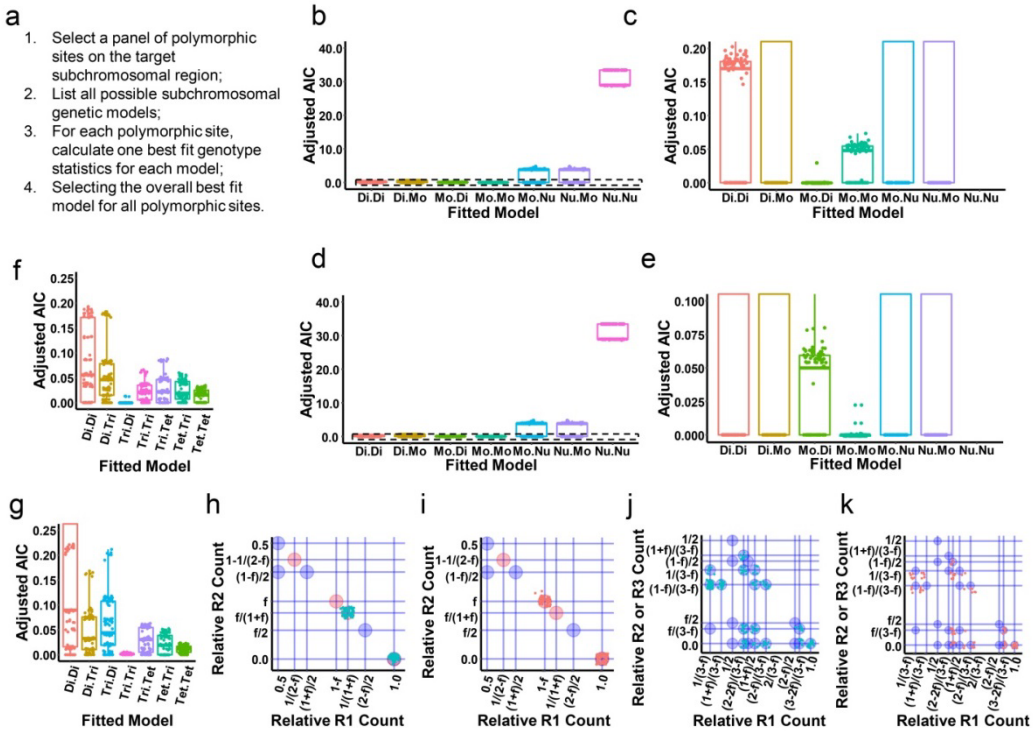

Fig. 4: Detection of fetal subchromosomal abnormality. a, Steps to detect subchromosomal abnormality using overall goodness-of-fit test for all polymorphic sites. **b-e,** Representative plots for detecting subchromosomal microdeletion of simulated chromosomes (**b, c**, simulated monosomy-disomy chromosome; **d, e**, simulated monosomy-monosomy chromosome) using overall goodness-of-fit tests. **c, e,** Partial enlarged drawings of **b** and **d**. **f, g,** Representative plots for detecting subchromosomal microduplication of simulated chromosomes (**f**, simulated trisomy-disomy chromosome; **g**, simulated trisomy-trisomy chromosome) using overall goodness-of-fit tests. **h, i**, Plotting over relative allelic clusters of subchromosomal deletion models for detecting maternal-fetal microdeletion (**h**, simulated monosomy-disomy chromosome; **i**, simulated monosomy-monosomy chromosome). **j, k**, Plotting over relative allelic clusters of some subchromosomal duplication models (fetal disomy model) for detecting maternal-fetal microduplication (**j**, simulated trisomy-disomy chromosome; **k**, simulated trisomy-trisomy chromosome). As there were allelic clusters not in the expected positions for a normal disomy fetus in plot **k**, either the fetus was abnormal for microduplications or the true and correct model was not included in the analysis.

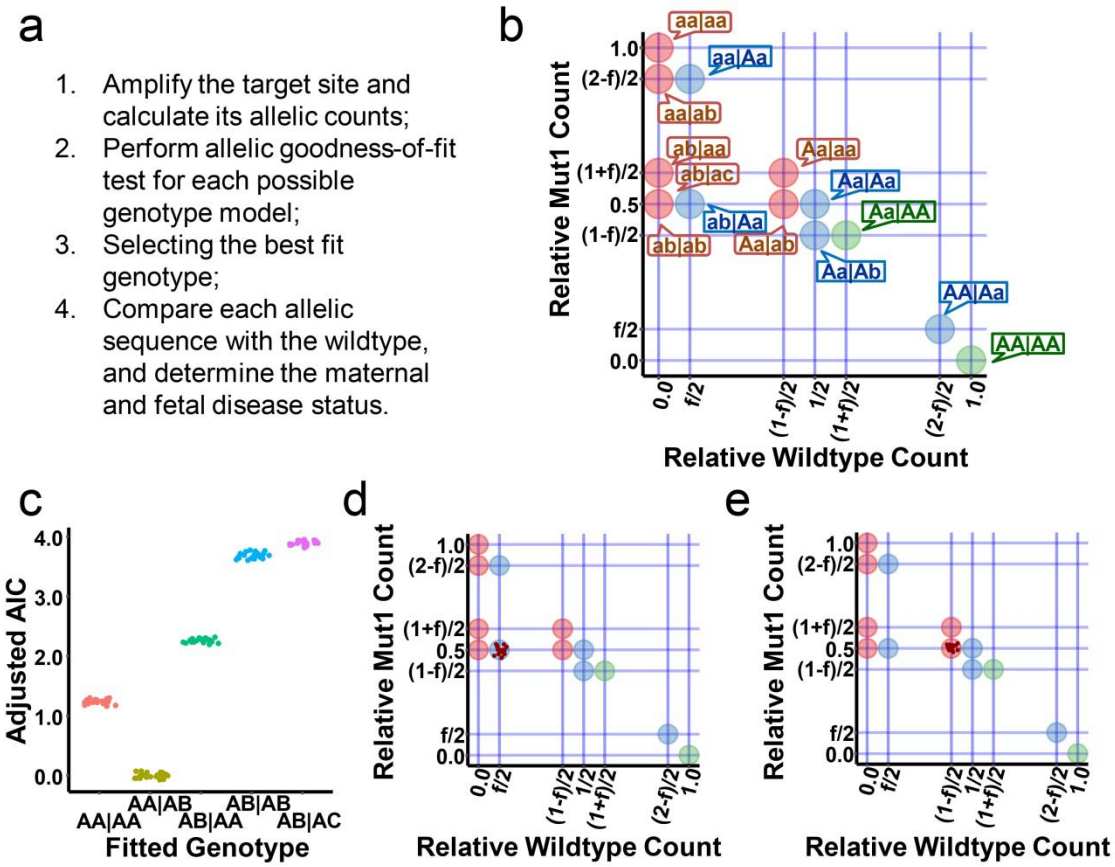

Fig. 5: Detection of fetal short genetic variations. a, Steps to detect sequence-level variation using goodness-of-fit test and wildtype sequence comparison. **b**, Expected all possible relative allelic clusters for polymorphic sites on normal disomy-disomy chromosomes (A, wildtype allele; a-c, different mutant alleles). **c**, Detection of short genetic variation by allelic goodness-of-fit analysis for a simulated site with library-level replicates. According to the plot, AA|AB genotype was the best fit. As allele A was mutant and allele B was wildtype by sequence analysis, the target was estimated to be a homozygous mutant-mutant for the mother and a heterozygous wildtype-mutant for the fetus. **d, e,** Plotting over relative allelic clusters of wildtype/mutant genotype models for detecting maternal-fetal short variation. According to the characteristic allelic positions, the simulated target site was estimated to be a heterozygous mutant-mutant for the mother and a heterozygous wildtype-mutant for the fetus (**d**) or a heterozygous wildtype-mutant for the mother and a heterozygous mutant-mutant for the fetus carrying two different mutant alleles (**e**).

Supplementary Figures

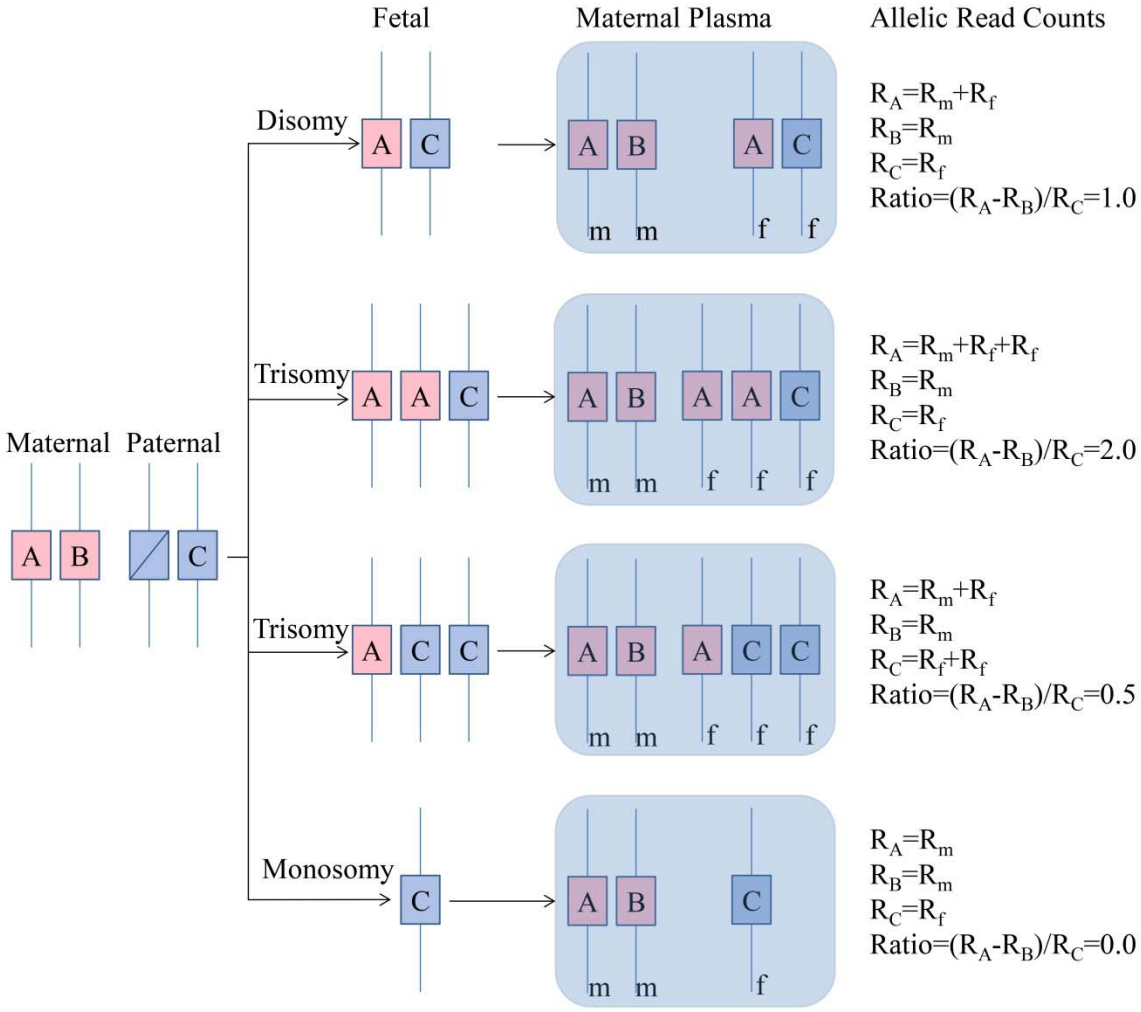

Fig. S1: Imbalance of allelic read counts for a polymorphic site from a heterozygous mother with a fetus inheriting a distinct allele from the father. A, B and C: distinct alleles for a polymorphic site; m and f: maternal and fetal genomic material; R_A, R_B and R_C: allelic read counts for alleles A, B and C, respectively.

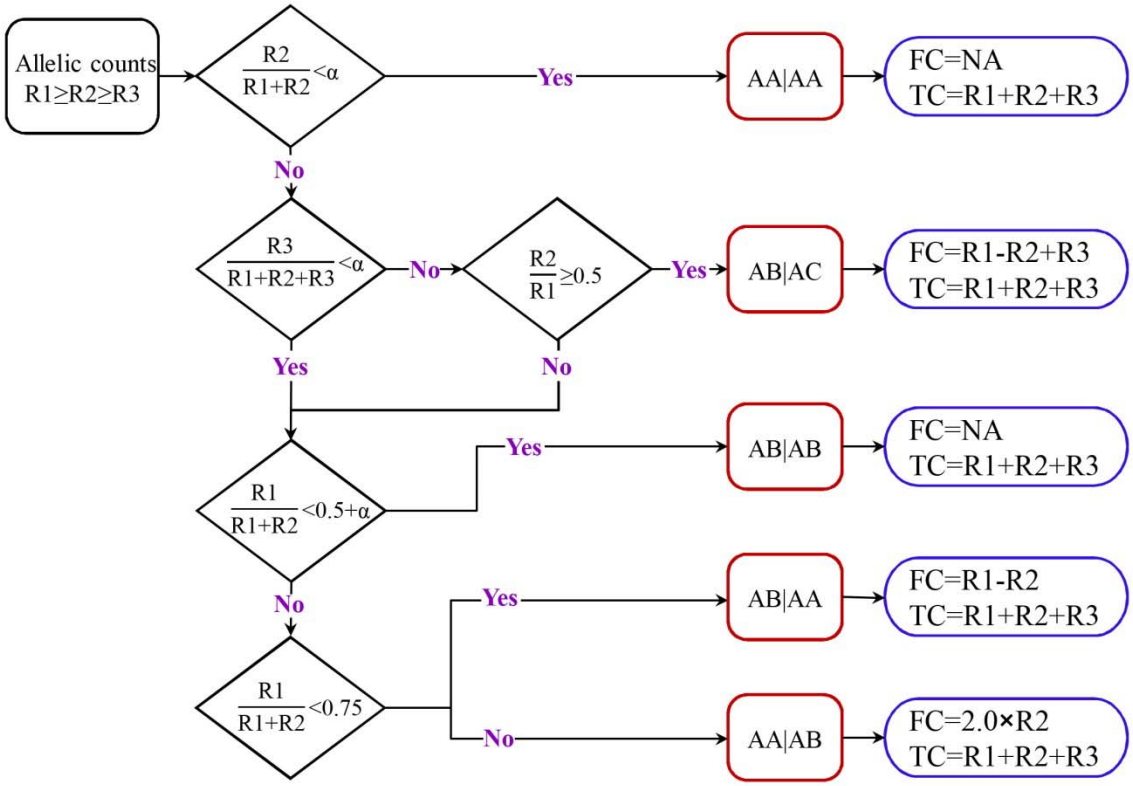

Fig. S2: Estimating the maternal-fetal genotype of a polymorphic site using its allelic read counts. R1, R2 and R3: allelic read counts in descending order; α: background noise threshold. A, B and C are distinct alleles for each polymorphic site, and the portion before the vertical bar denotes the maternal genotype and the part after the vertical bar denotes the fetal genotype. FC: estimated reads count amplified from fetal genetic materials (Fetal Reads); TC: total reads count amplified from both maternal and fetal genetic materials (Total Reads).

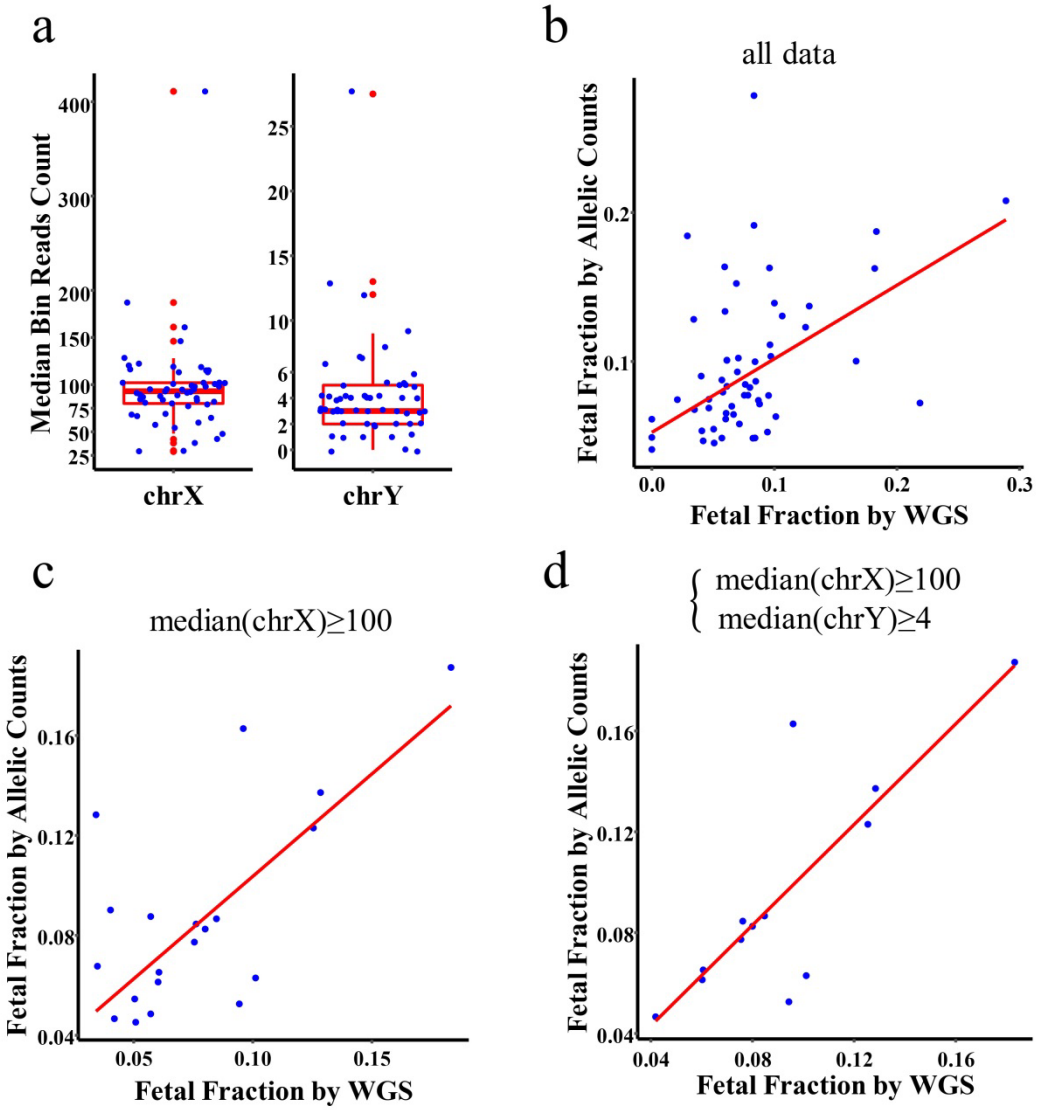

Fig. S3: Fetal fraction estimation using allelic read counts or whole genome sequencing. a, Median bin read counts for WGS dataset of the insertion/deletion polymorphism samples. **b-d**, Fetal fractions were estimated for each sample by both allelic read counts and WGS methods, and their relationship was plotted (red line was the fitted regression line y~x; **b**, all samples; **c**, excluding WGS samples with bin read counts<100; **d**, same as Fig. 1e, included here for comparison purposes). WGS: whole genome sequencing.

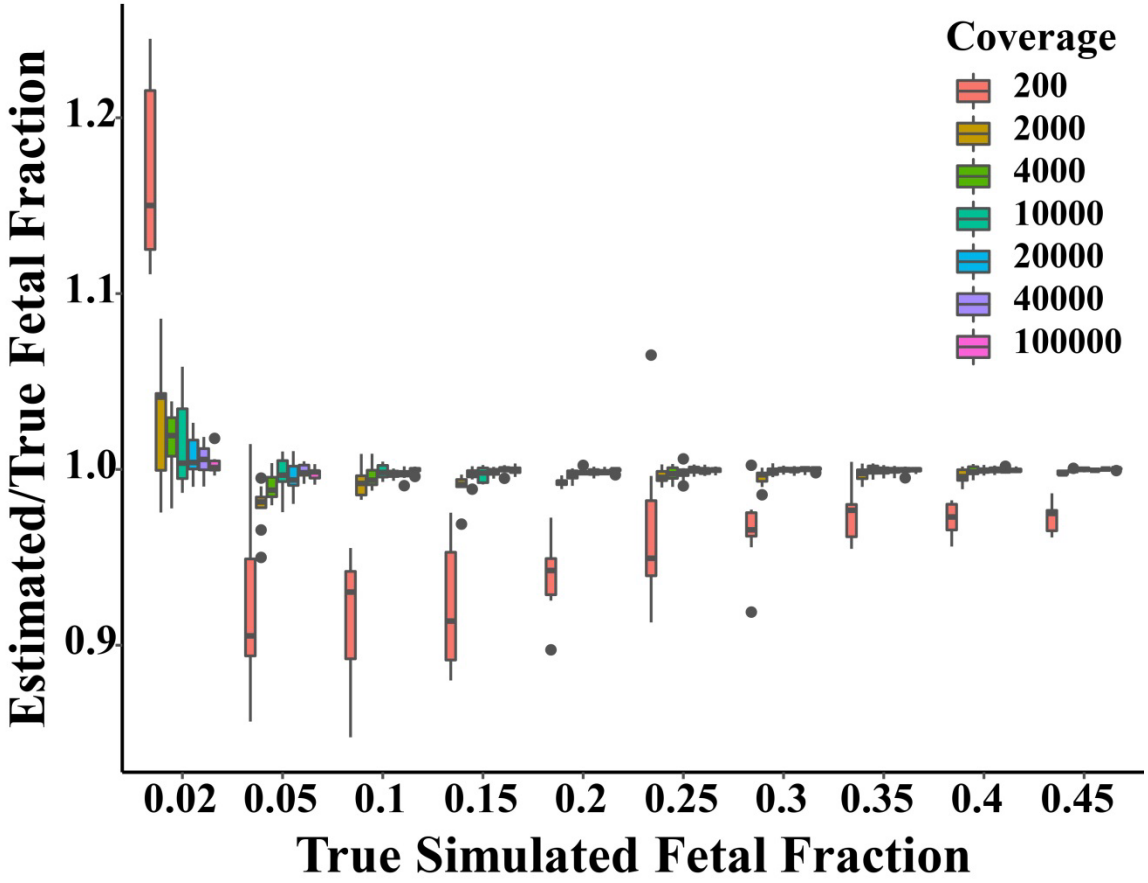

Fig. S4: Estimation accuracy for fetal fractions of simulated samples. One hundred samples were simulated for each sequencing coverage, and 100 polymorphic sites were simulated for each sample. At each polymorphic site, allelic sequences for one of the five disomic-disomic genotypes were randomly generated with different fetal fractions. Fetal fraction for each sample was estimated using allelic reads counts. The ratio of the estimated fetal fraction to the true fetal fraction (the simulated value) was plotted and grouped by sequencing coverage.

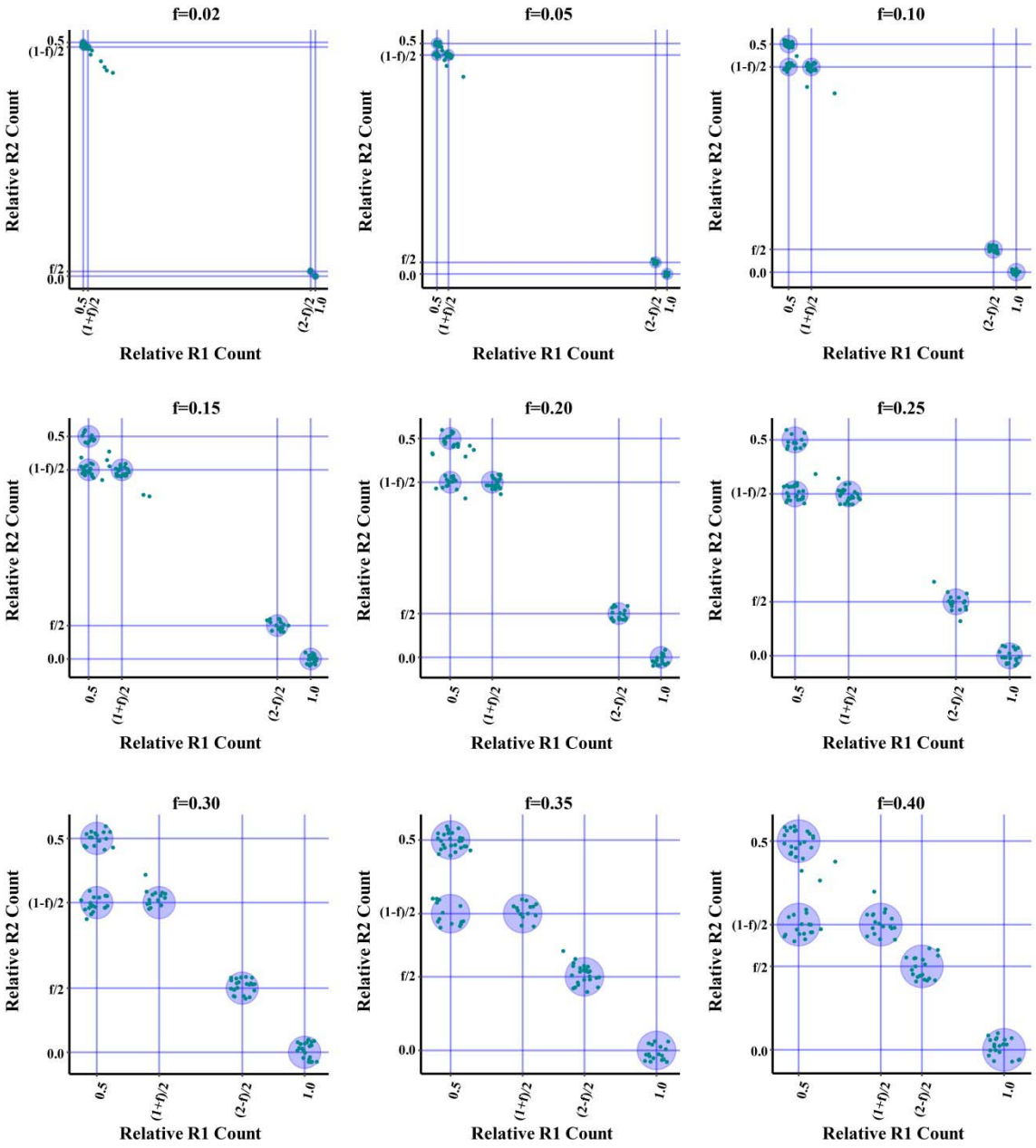

Fig. S5: Distribution plots of relative allelic counts. One hundred polymorphic sites on a disomy-disomy chromosome were simulated for each sample. For each polymorphic site in a sample, relative allelic read counts were calculated, and then the relative R2 count was plotted against the relative R1 count. One representative plot was shown for each fetal fraction. f: fetal fraction. Relative R1 Count=R1/(R1+R2+R3) and Relative R2 Count=R2/(R1+R2+R3).

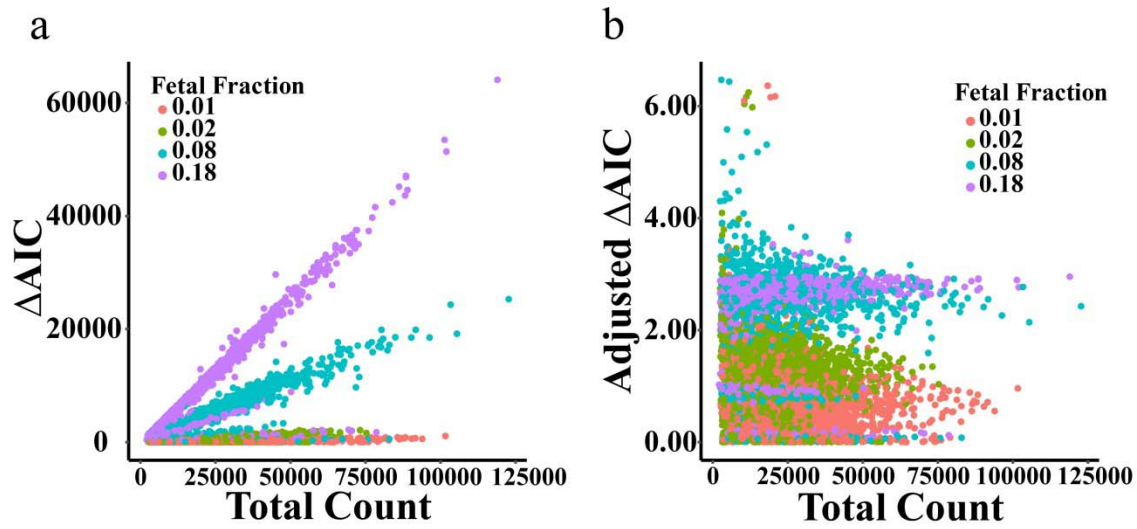

Fig. S6: Influence of fetal fraction and total allelic read count on ΔAIC. Fetal fraction was estimated for each sample in the replicates dataset and rounded to the second decimal place. **a,** Absolute ΔAIC was calculated for each polymorphic site of the replicate samples using the disomic-disomic model, plotted against total allelic read count and grouped by the estimated fetal fraction. **b**, Absolute adjusted ΔAICs were calculated for the replicate samples and plotted against total allelic read counts.

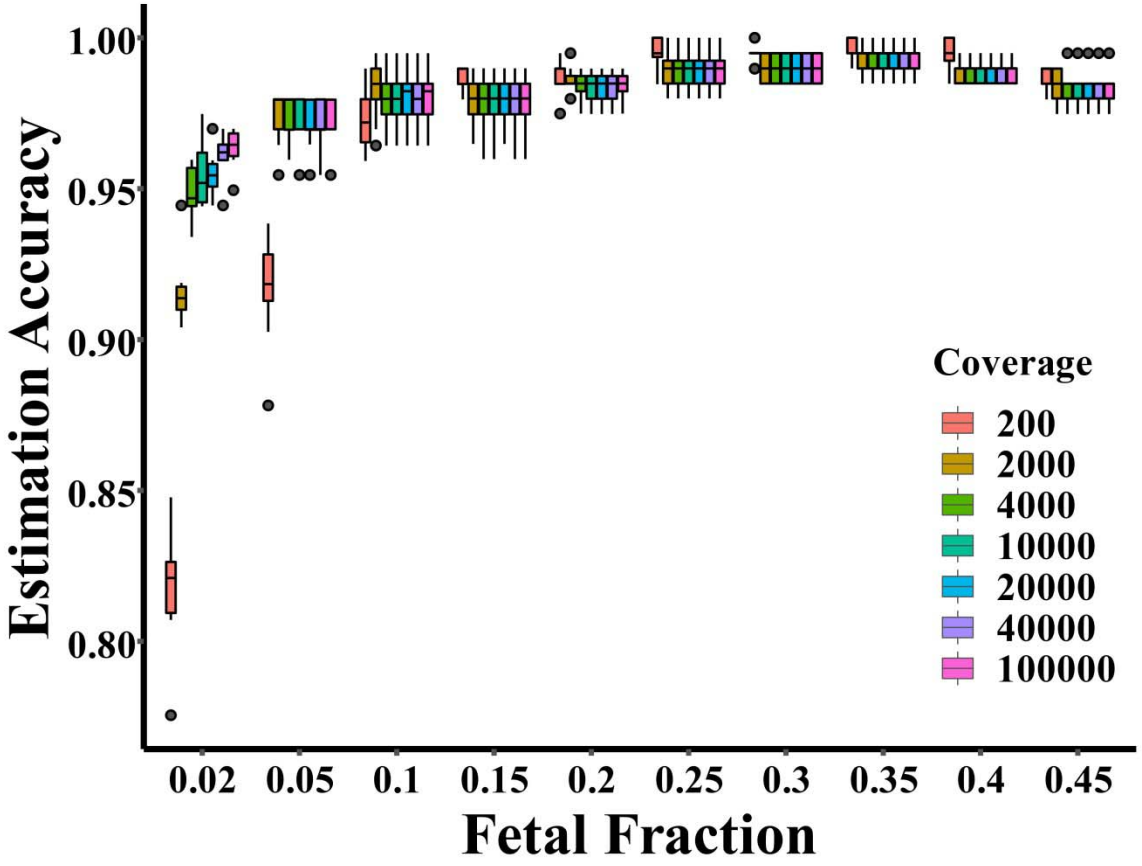

Fig. S7: Influence of fetal fraction on maternal-fetal genotype estimation. Sequencing reads were simulated for samples with different fetal fractions and different sequencing coverage, and fetal fraction was estimated for each sample followed with genotype estimation for each polymorphic site. Estimation accuracy was calculated as the ratio of the number of correctly estimated genotypes to the total number of all polymorphic sites, and then plotted against fetal fraction grouped by sequencing coverage.

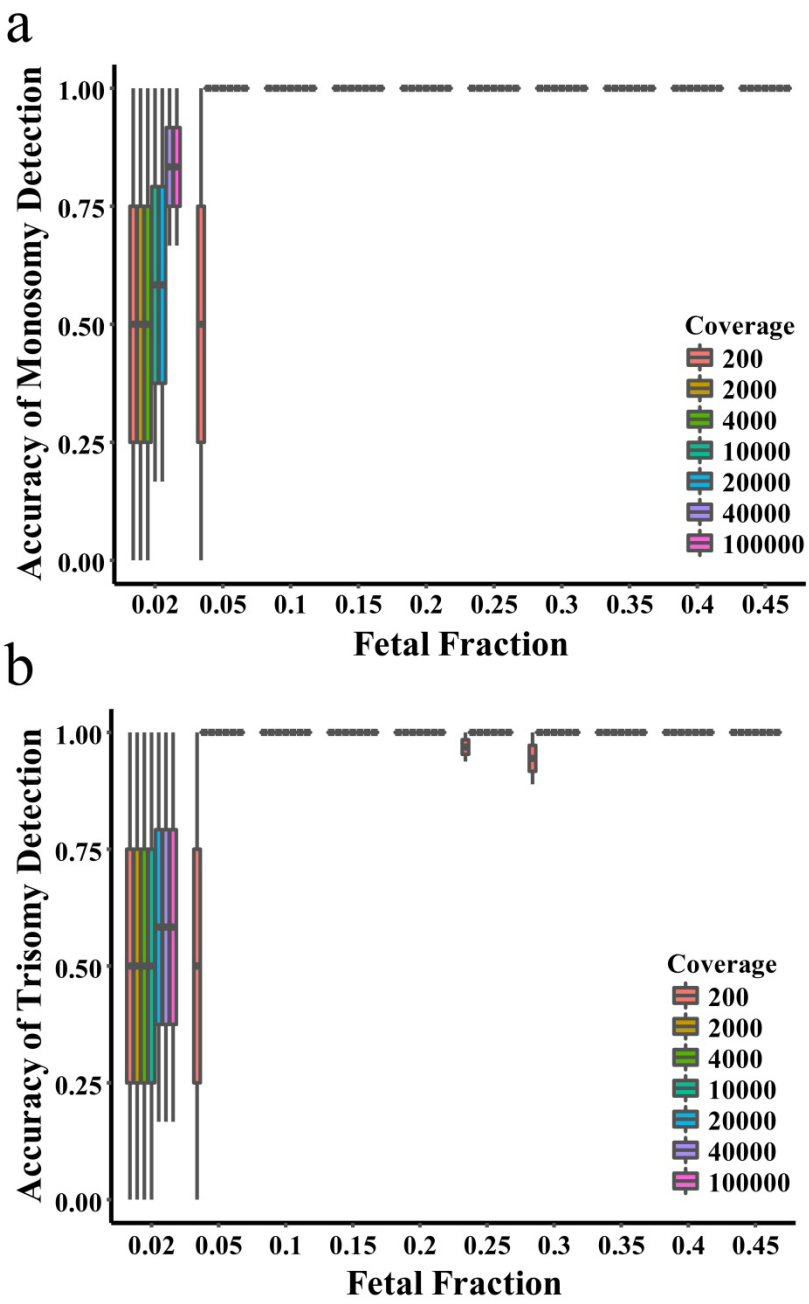

Fig. S8: Detecting accuracy for chromosomal aneuploidies. a, In each sample, one disomy-disomy chromosome and one disomy-monosomy chromosome were simulated. Chromosomal aneuploidy for each chromosome in each sample was estimated using overall allelic goodness-of-fit test. One hundred samples with different fetal fractions were simulated for each sequencing coverage. **b,** In each sample, one disomy-disomy chromosome and one disomy-trisomy chromosome were simulated. Chromosomal aneuploidy for each chromosome in each sample was estimated using overall allelic goodness-of-fit test. One hundred samples with different fetal fractions were simulated for each sequencing coverage.

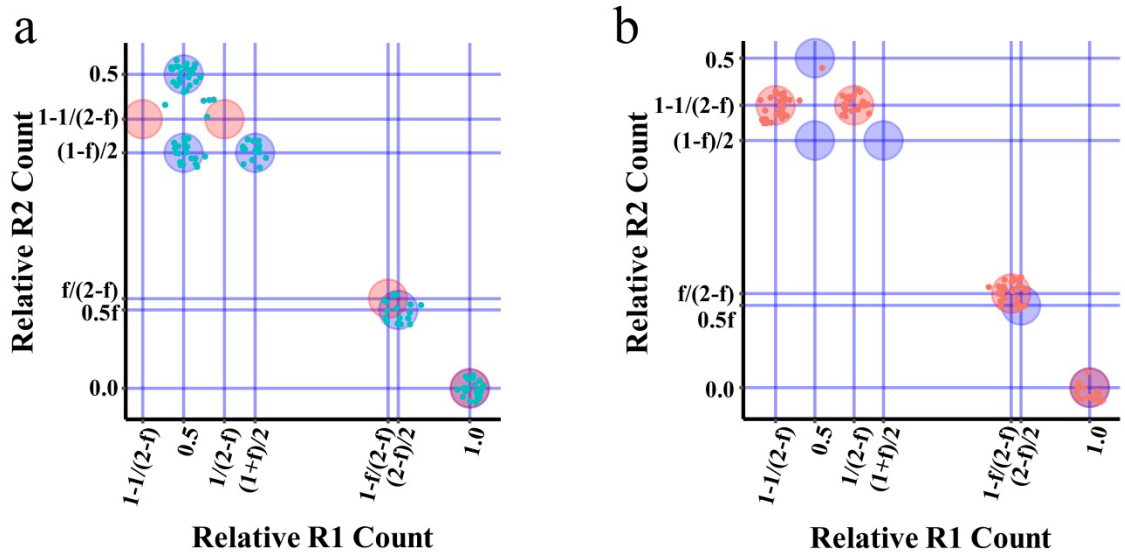

Fig. S9: Detection of chromosomal monosomy. a, Relative allelic count plot for simulated polymorphic sites on a representative target chromosome. From the characteristic cluster positions, the target chromosome was estimated to be disomy-disomy. **b**, Relative allelic count plot for simulated polymorphic sites on a representative target chromosome. From the characteristic cluster positions, the target chromosome was estimated to be disomy-monosomy. f: fetal fraction.

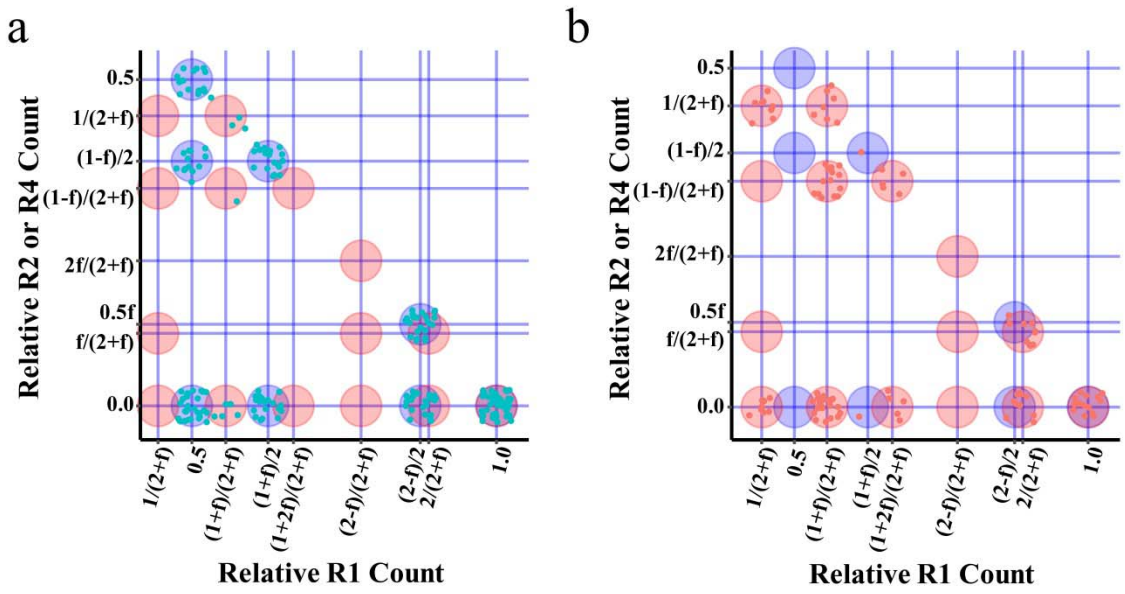

Fig. S10: Detection of chromosomal trisomy. a, Relative allelic count plot for simulated polymorphic sites on a representative target chromosome. From the characteristic cluster positions, the target chromosome was estimated to be disomy-disomy. **b**, Relative allelic count plot for simulated polymorphic sites on a representative target chromosome. From the characteristic cluster positions, the target chromosome was estimated to be disomy-trisomy.

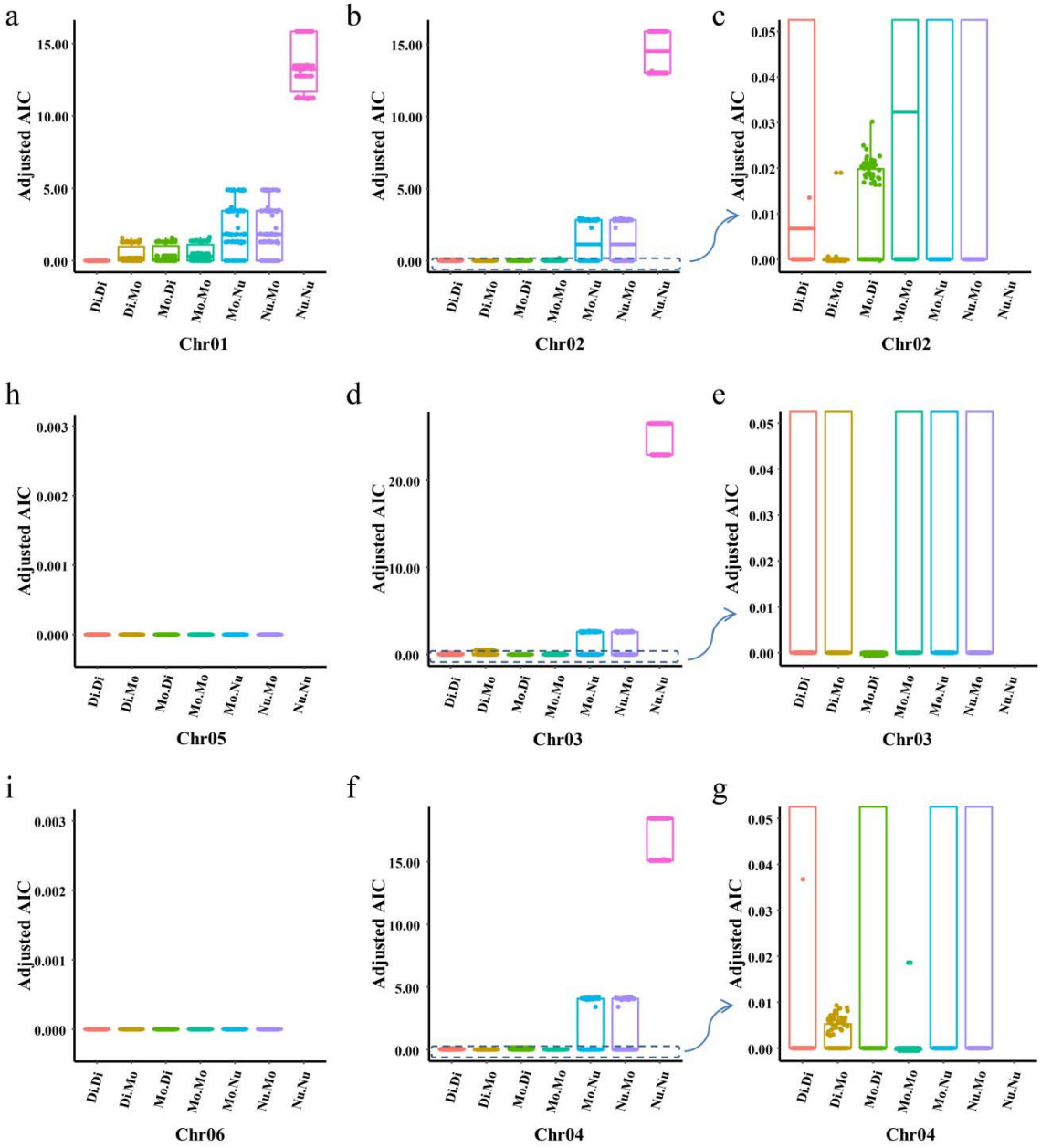

Fig. S11: Detection of subchromosomal deletion. Maternal-fetal chromosomes (labeled as Chr01-Chr06) were simulated, and each having 100 polymorphic sites. Chr01-Chr06 chromosomes were simulated as disomy-disomy (Di.Di), disomy-monosomy (Di.Mo), monosomy-disomy (Mo.Di), monosomy-monosomy(Mo.Mo), monosomy-nullisomy (Mo.Nu) and nullisomy-monosomy (Nu.Mo), respectively. Allelic read counts of each polymorphic site was tested against all possible genotypes assuming each one of the seven maternal-fetal chromosomal models (Di.Di, Di.Mo, Mo.Di, Mo.Mo, Mo.Nu, Nu.Mo and Nu.Nu), and the overall best fitted model for all target polymorphic sites was selected for each chromosome. **a,b,d,f,h,i**, Overall fitted results for each chromosome. **c,e,g**, Partial enlarged drawings of **b**, **d** and **f**, respectively.

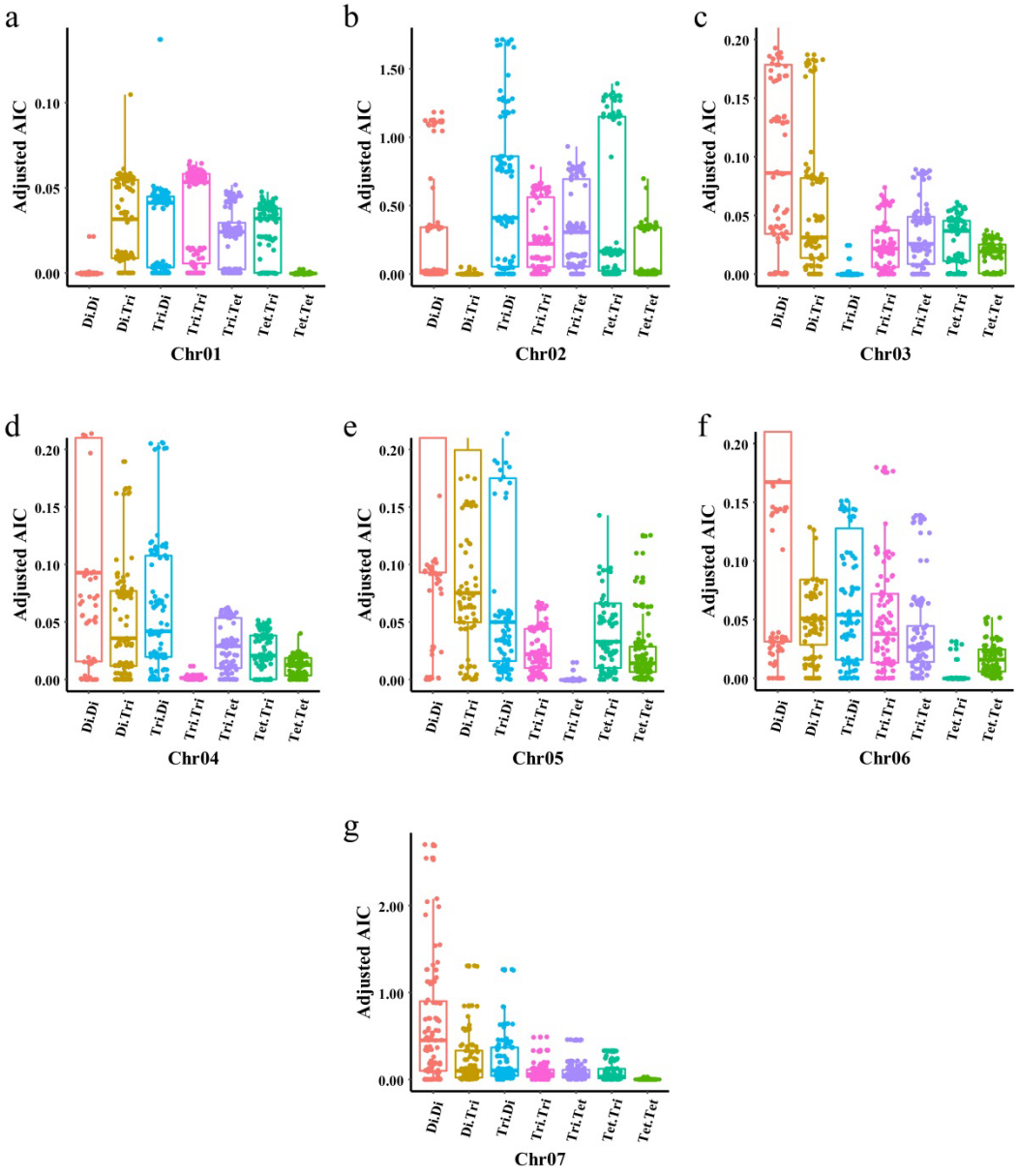

Fig. S12: Detection of subchromosomal duplication. Maternal-fetal chromosomes (labeled as Chr01-Chr07) were simulated, and each having 100 polymorphic sites. Chr01-Chr07 chromosomes were simulated as disomy-disomy (Di.Di), disomy-trisomy (Di.Tri), trisomy-disomy (Tri.Di), trisomy-trisomy (Tri.Tri), trisomy-tetrasomy (Tri.Tet), tetrasomy-trisomy (Tet.Tri) and tetrasomy-tetrasomy(Tet.Tet), respectively. Allelic read counts of each polymorphic site was tested against all possible genotypes assuming each one of the seven maternal-fetal chromosomal models (Di.Di, Di.Tri, Tri.Di, Tri.Tri, Tri.Tet, Tet.Tri and Tet.Tet), and the overall best fitted model for all target polymorphic sites was selected for each chromosome. **a,b,g**, Overall fitted results for chromosomes Chr01, Chr02 and Chr07, respectively. **c,d,e,f**, Partial enlarged drawings of overall fitted results for chromosomes Chr03, Chr04, Chr05 and Chr06, respectively.

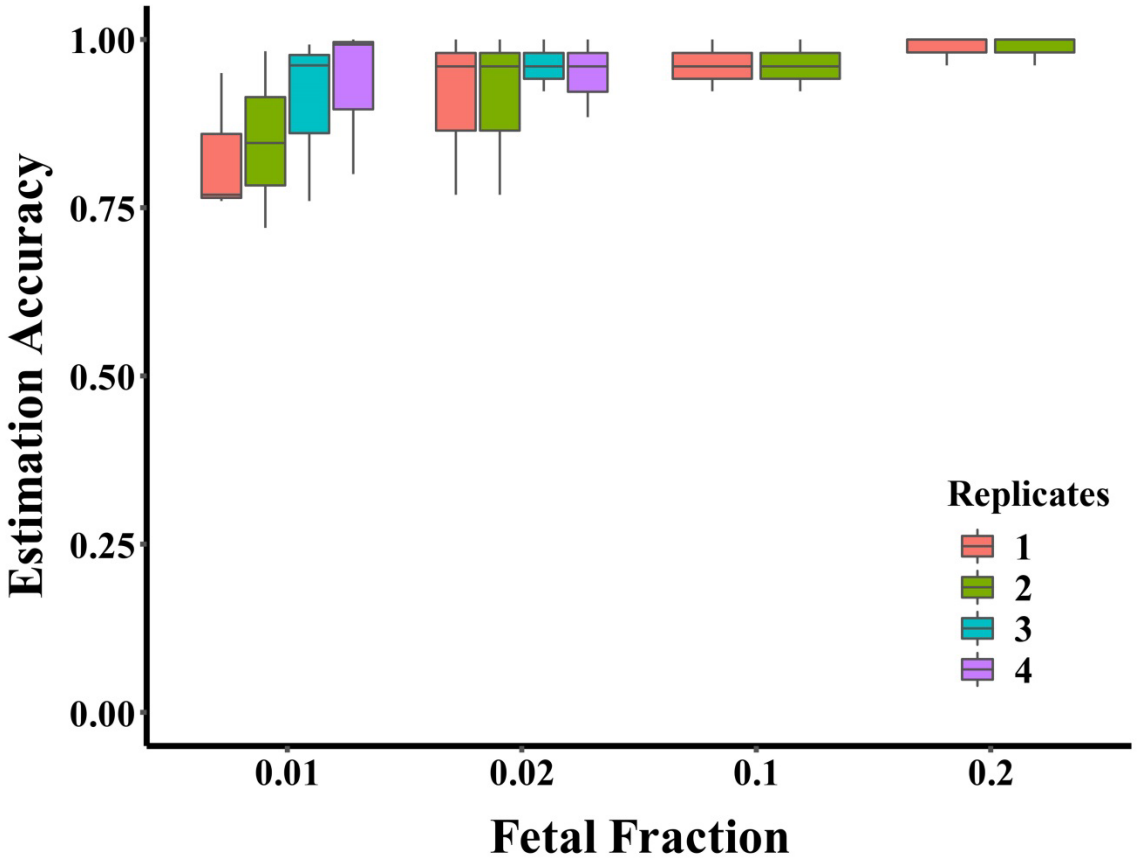

Fig. S13: Genotype estimation accuracy for the replication dataset. Genotype was estimated for each polymorphic site using its allelic read counts for each sample in the replication dataset. Estimation accuracy was calculated as the ratios of the number of correctly estimated genotypes to the total number of polymorphic sites grouped by different replicates and different fetal fractions. Replicates were labeled as 1 to 4, and ratios for replicates 1 to 4 means that 1 to 4 samples were used to calculate the estimation accuracy, respectively.

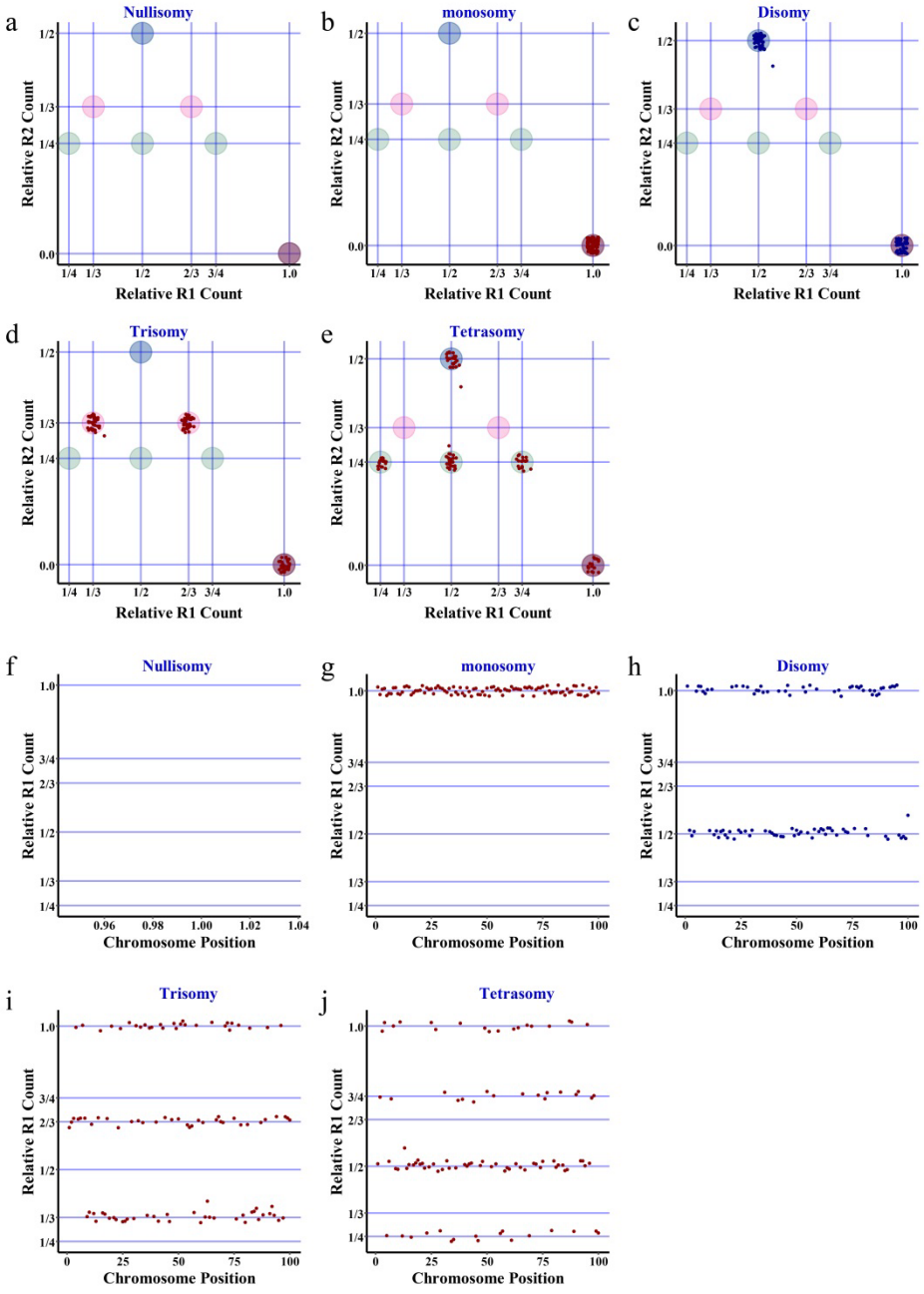

Fig. S14: Detecting genetic aberrations for samples from non-pregnant individuals or preimplantation embryos. A panel of polymorphic sites on the target chromosome was simulated for a normal non-pregnant individual, and relative allelic counts for each polymorphic site were calculated. Then the relative R2 count was plotted against the relative R1 count (**a-e**) or the relative R1 count was plotted against its relative chromosomal position (**f-j**) for each amplicon. **a, f**, nullisomy (or homozygous microdeletion); **b, g**, monosomy (or heterozygous microdeletion); **c, h**, disomy (or normal); **d, i**, trisomy (or heterozygous microduplication); **e, j**, tetrasomy (or homozygous microduplication).

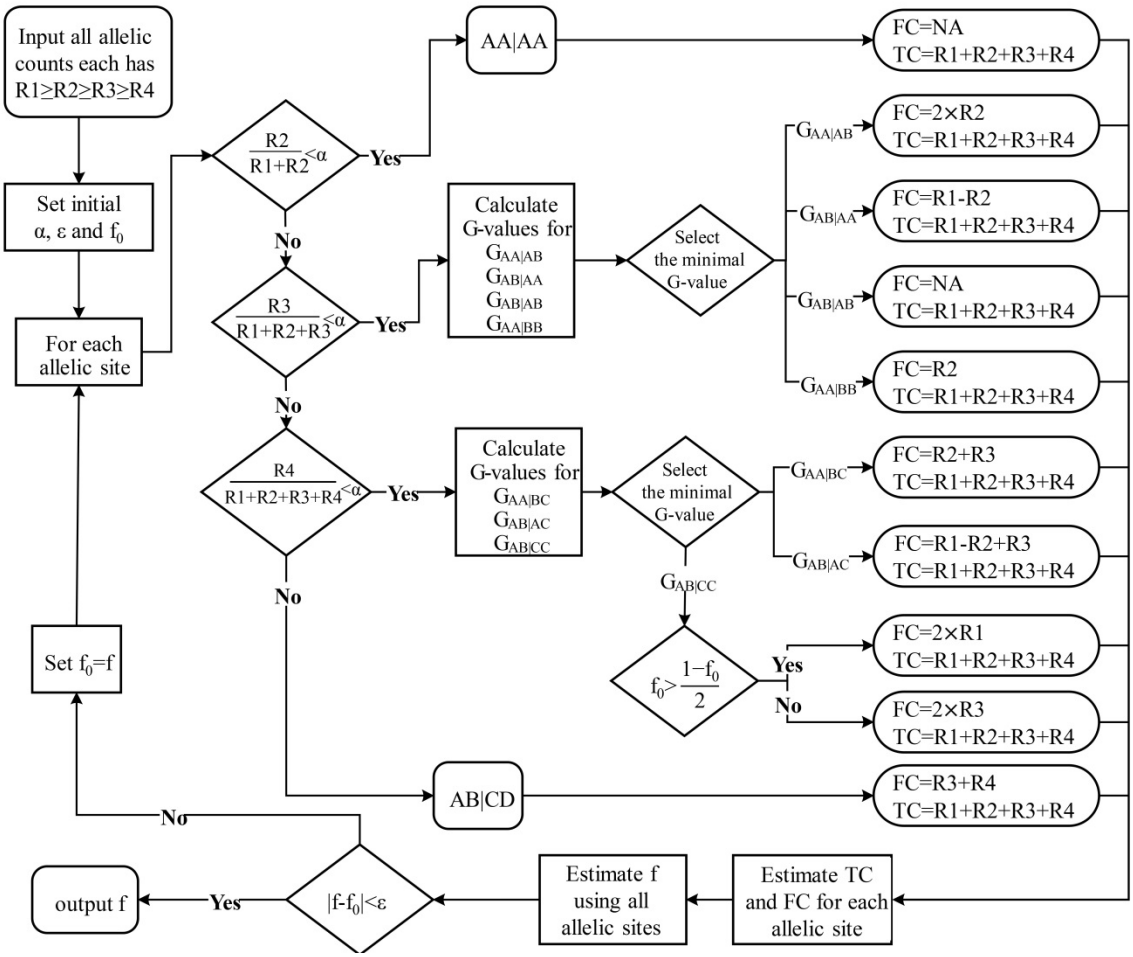

Fig. S15: Estimating fetal fraction for a sample from a surrogate mother using allelic read counts. R1, R2, R3 and R4: allelic read counts in descending order; α: background noise threshold; ε: estimation precision; f_0: initial fetal fraction estimate; A-D: distinct alleles for each polymorphic site.

Supplementary Tables

Table S1: Relative Allelic Counts for a Polymorphic Site on Reference Chromosomes

Genotype	Allelic Read Counts			R1/(R1+R2)	Estimation	
	R1	R2	R3		Fetal Reads	Total Reads
AA|AA	$R_mR_mR_fR_f$	0	0	1	NA	R1
AA|AB	$R_mR_mR_f$	R_f	0	1-0.5*f∈ (0.75, 1)	2.0*R2	R1+R2
AB|AA	$R_mR_fR_f$	R_m	0	0.5+0.5*f∈ (0.5, 0.75]	R1-R2	R1+R2
AB|AB	R_mR_f	R_mR_f	0	0.5	NA	R1+R2
AB|AC	R_mR_f	R_m	R_f	1/(2-f)∈ [0.5, 2/3]	R1-R2+R3	R1+R2+R3

1. f: fetal fraction
2. R1, R2 and R3: read counts of each allele sorted in descending order
3. R_m and R_f: Reads mapped to maternal and fetal chromosomes, respectively.

Table S2: Relative Allelic Count for Disomy-Disomy Model

Genotype	RRC1	RRC2	RRC3
AA|AA	1	0	0
AA|AB	(2-f)/2	f/2	0
AB|AA	(1+f)/2	(1-f)/2	0
AB|AB	1/2	1/2	0
AB|AC	1/2	(1-f)/2	f/2

1. RRC1 (relative R1 count)=R1/(R1+R2+R3)
2. RRC2 (relative R2 count)=R2/(R1+R2+R3)
2. RRC3 (relative R3 count)=R3/(R1+R2+R3)

Table S3: Relative Allelic Count for Disomy-Monosomy Model

Genotype	RRC1	RRC2	RRC3
AA|AØ	1	0	0
AA|BØ	1-f/(2-f)	f/(2-f)	0
AB|AØ	1/(2-f)	1-1/(2-f)	0
AB|CØ	1-1/(2-f)	1-1/(2-f)	f/(2-f)

1. RRC1 (relative R1 count)=R1/(R1+R2+R3)
2. RRC2 (relative R2 count)=R2/(R1+R2+R3)
2. RRC3 (relative R3 count)=R3/(R1+R2+R3)

Table S4: Relative Allelic Count for Disomy-Trisomy Model

Genotype	RRC1	RRC2	RRC3	RRC4
AA|AAA	1	0	0	0
AA|AAB	2/(2+f)	f/(2+f)	0	0
AA|ABB	(2-f)/(2+f)	2f/(2+f)	0	0
AB|AAA	(1+2f)/(2+f)	(1-f)/(2+f)	0	0
AB|AAB	(1+f)/(2+f)	1/(2+f)	0	0
AA|ABC	(2-f)/(2+f)	f/(2+f)	f/(2+f)	0
AB|AAC	(1+f)/(2+f)	(1-f)/(2+f)	f/(2+f)	0
AB|ABC	1/(2+f)	1/(2+f)	f/(2+f)	0
AB|ACC	1/(2+f)	(1-f)/(2+f)	2f/(2+f)	0
AB|ACD	1/(2+f)	(1-f)/(2+f)	f/(2+f)	f/(2+f)

1. RRC1 (relative R1 count)=R1/(R1+R2+R3+R4)
2. RRC2 (relative R2 count)=R2/(R1+R2+R3+R4)
3. RRC3 (relative R3 count)=R3/(R1+R2+R3+R4)
4. RRC4 (relative R4 count)=R4/(R1+R2+R3+R4)

Table S5: Relative Allelic Count for Subchromosomal Microdeletion Model

Genotype		RRC1	RRC2
Di.Mo	AA|AØ	1	0
	AB|AØ	1/(2-f)	(1-f)/(2-f)
Mo.Di	AØ|AA	1	0
	AØ|AB	1/(1+f)	f/(1+f)
Mo.Mo	AØ|AØ	1	0
	AØ|BØ	1-f	f
Nu.Mo	ØØ|AØ	1	0
Mo.Nu	ØA|ØØ	1	0
Nu.Nu	ØØ|ØØ	0	0

1. RRC1 (relative R1 count)=R1/(R1+R2+R3)
2. RRC2 (relative R2 count)=R2/(R1+R2+R3)
3. Only heritable genotypes were listed.

Table S6: Relative Allelic Count for Subchromosomal Microduplication Model

Genotype		RRC1	RRC2	RRC3	RRC4
Trisomy-Disomy Model	AAA|AA	1	0	0	0
	AAA|AB	(3-2f)/(3-f)	f/(3-f)	0	0
	AAB|AA	2/(3-f)	(1-f)/(3-f)	0	0
	AAB|AB	(2-f)/(3-f)	1/(3-f)	0	0
	AAB|BB	(2-2f)/(3-f)	(1+f)/(3-f)	0	0
	AAB|AC	(2-f)/(3-f)	(1-f)/(3-f)	f/(3-f)	0
	AAB|BC	(2-2f)/(3-f)	1/(3-f)	f/(3-f)	0
	ABC|AA	(1+f)/(3-f)	(1-f)/(3-f)	(1-f)/(3-f)	0
	ABC|AB	1/(3-f)	1/(3-f)	f/(3-f)	0
	ABC|AD	1/(3-f)	(1-f)/(3-f)	(1-f)/(3-f)	f/(3-f)
Other Genotypes		…	…	…	…

1. Only the model having normal fetal genotypes is listed.

Table S7: Genotype estimation for a two-allele site

Group	R1's Allele	R2's Allele	Expected Genotype	Relative Read Count	
				Wildtype	Mutant
I	A		AA|AA	1	0
(AA|AA)	a		aa|aa	0	1
II	A	a	AA|Aa	(2-f)/2	f/2
(AA|AB)	a	A	aa|Aa	f/2	(2-f)/2
III	A	a	Aa|AA	(1+f)/2	(1-f)/2
(AB|AA)	a	A	Aa|aa	(1-f)/2	(1+f)/2
IV	A	a	Aa|Aa	1/2	1/2
(AB|AB)	a	A	Aa|Aa	1/2	1/2

1. Group: estimated genotype groups by allelic read counts.
2. A and a: wildtype and mutant alleles for a polymorphic site

Table S8: Genotype estimation for a site with more than two alleles

Group	R1's Allele	R2's Allele	R3's Allele	Expected Genotype	Relative Read Count		
					Wildtype	Mutant 1	Mutant 2
I (AA|AA)	A			AA|AA	1	0	0
	a			aa|aa	0	1	0
II (AA|AB)	A	a		AA|Aa	(2-f)/2	f/2	0
	a	A		aa|Aa	f/2	(2-f)/2	0
	a	b		aa|ab	0	(2-f)/2	f/2
III (AB|AA)	A	a		Aa|AA	(1+f)/2	(1-f)/2	0
	a	A		Aa|aa	(1-f)/2	(1+f)/2	0
	a	b		ab|aa	0	(1+f)/2	(1-f)/2
IV (AB|AB)	A	a		Aa|Aa	1/2	1/2	0
	a	A		Aa|Aa	1/2	1/2	0
	a	b		ab|ab	0	1/2	1/2
V (AB|AC)	A	a	b	Aa|Ab	1/2	(1-f)/2	f/2
	a	A	b	Aa|ab	(1-f)/2	1/2	f/2
	a	b	A	ab|Aa	f/2	1/2	(1-f)/2
	a	b	c	ab|ac	0	1/2	(1-f)/2

1. Group: estimated genotype groups by allelic read counts. A-C: different alleles.
2. A and a-c: wildtype and mutant alleles for a polymorphic site

Supplementary Methods

Dataset:

The insertion/deletion polymorphism dataset (BioProject ID: PRJNA387652): A panel of 44 biallelic insertion/deletion polymorphic sites plus *ZFX/ZFY* was amplified using cfDNA or maternal genomic DNA as template. Some of the cfDNA samples were also sequenced using low coverage whole genome sequencing.

The replication dataset (BioProject ID: PRJNA517742): Genomic DNAs from two independent blood samples were mixed generating samples with minor allele frequencies of 0.5%, 1.0%, 5% and 10%, respectively. Mixed samples were PCR amplified using 564 primer pairs and sequenced.

The simulated datasets: Five hundred random 70-bp amplicon sequences were generated, and specific mutations were introduced into each amplicon to simulate polymorphic sites having four to six alleles each and could be identified by at least two unique 12-mer indexes. Fetal fraction in each sample was simulated as one of the following values: 0.02, 0.05, 0.10, 0.15, 0.20, 0.25, 0.30, 0.35, 0.40 and 0.45. In each simulated sample, a total of 400 polymorphic sites were selected and each had 200 genomic copies. Each polymorphic site was assigned to be one of the possible maternal-fetal genotypes randomly, and different number of allelic sequence amplicons was generated. For example, if the fetal fraction was 0.05, and the genotype was “AB|AC”, 100 copies of allele seqA, 95 copies of allele seqB and 5 copies of allele seqC were produced as amplicon templates for a polymorphic site having the genotype AB|AC. After generating amplicon templates for all of the polymorphic sites in a sample, sequencing reads were simulated using the ART simulator with the following command “art_illumina -ss HSXt -amp -i <inputfile> -na -l 65 -f <fold> -o <outputfile>”.

Reads Processing and Mapping

Reads retrieved from SRA or simulated were filtered out using custom scripts as follows. For each read, base positions with a quality score of 14 or less were identified, and then the longest subsequence was selected whereas each base in the subsequence had a quality score greater than 14. Subsequently, filtered reads were mapped first to unique polymorphic sites using 12-mer indexes, and then each read was mapped to a specific allele using unique allelic indexes. Finally, different alleles were counted for each polymorphic site in each sample.

Fetal Fraction Estimation

For each polymorphic site, read counts for all alleles were sorted in descending order and labeled as R1, R2, R3, etc., and the allelic read count Ri was considered as a noise background if its relative value ($RRi = Ri/\sum_{j=1}^{i} R_j$) was less than the background threshold (α). All polymorphic sites used for fetal fraction estimation were assumed to be one of the normal disomy-disomy maternal-fetal genotypes (AA|AA, AA|AB, AB|AA, AB|AB or AB|AC, where the portion before the vertical bar denotes the maternal genotype and the portion after it denotes the fetal genotype), as the majority of the polymorphic sites were from chromosomes that were normal and only a

small portion of them were abnormal if any at all. For each polymorphic site from a reference normal disomy-disomy chromosome, there are at most three informative alleles exist. In an ideal situation, if one or three alleles are detected for a target site, then its genotype can be determined unambiguously, while if two alleles are detected, a single measure of R1/(R1+R2) was informative enough to classify all three possible genotypes as follows. If the genotype is AA|AB, then R1/(R1+R2)=1-0.5f, where f denotes fetal fraction. As f is the minor component and f<0.5, then 1-0.5f ≥ 0.75. If the genotype is AB|AA, then R1/(R1+R2)=0.5+0.5f. As f<0.5, then must 0.5+0.5f ≤ 0.75. If the genotype is AB|AB, then R1/(R1+R2)=0.5 irrespective of f values. Therefore, for each polymorphic site (Fig. S2, RR2=R2/(R1+R2) and RR3=R3/(R1+R2+R3)), if only one informative allele was detected (RR2<α), then the genotype would be AA|AA. If two informative alleles were present (RR2≥α and RR3<α), then the site should be one of the genotypes having two different alleles (AA|AB, AB|AA or AB|AB), which could be identified using the ratio $R1/(R1 + R2)$ as follows: when the ratio ≥0.75, the genotype was estimated to be AA|AB, between 0.5+α and 0.75 to be AB|AA and between 0.5 and 0.5+α to be AB|AB. If three alleles were informative (RR3≥α), then the genotype was AB|AC if R2/R1≥0.5, and R3 was considered as a background noise outlier otherwise. Clearly, relative allelic read counts of three genotypes were affected by the sample's fetal fraction, and the estimated read count derived from fetal genetic materials (FC, FetalReads) was calculated along with the total read count (TC, TotalReads) for each polymorphic site (Fig. S2, Table S1). Finally, the fetal read counts (FetalReads) were regressed against the total read counts (TotalReads) for a panel of polymorphic sites using the R's rlm function in MASS package with the fitting model $y = \beta x + 0$, and fetal fraction was estimated as the model coefficient (β).

For example, the following are imaginary representative allelic read counts for five polymorphic sites from a sample (R1-R3: allelic read counts in descending order). Background α is set to 0.01.

MarkerID	R1	R2	R3
ID-01	14127	35	0
ID-02	4105	577	13
ID-03	3148	3101	54
ID-04	5809	3552	27
ID-05	4007	3028	1011

For ID-01, RR2=R2/(R1+R2)=35/(14127+35)=0.002<0.01, genotype is AA|AA.
FetalReads=NA. TotalReads=R1 =14127.

For ID-02, RR2=R2/(R1+R2)=577/(4105+577)=0.123≥0.01 and
RR3=R3/(R1+R2+R3)=13/(4105+577+13)=0.003<0.01, two alleles are informative.
Ratio=R1/(R1+R2)=0.877. As Ratio≥0.75, genotype is AA|AB.
FetalReads=2 × R2=2×577=1154. TotalReads=R1+R2=4682.

For ID-03, RR2=0.496≥0.01 and RR3=0.009<0.01, two alleles are informative. Ratio=0.504. As 0.5≤Ratio<0.51, genotype is AB|AB.
FetalReads=NA. TotalReads=R1+R2=6249.

For ID-04, RR2=0.379≥0.01, and RR3=0.003<0.01, two alleles are informative. Ratio=0.621. As 0.51≤Ratio<0.75, genotype is AB|AA.
FetalReads=R1-R2 =2257, TotalReads=R1+R2=9361.

For ID-05, RR2=0.430≥0.01, and RR3=0.126>0.01, three alleles are informative. As R2/R1=0.756≥0.5, genotype is AB|AC.
FetalReads=R1-R2+R3=1990, TotalReads=R1+R2+R3=8046.

Three polymorphic sites are considered informative for fetal fraction estimation in the above sample (ID-02, ID-04 and ID-05). Hence a robust linear regression model is fitted using the three informative sites and the fetal fraction (f) is estimated by the following R commands:

```
FetalReads=c(NA,1154,NA,2257,1990)
TotalReads=c(14127,4682,6249,9361,8046)
rlmfit=rlm(FetalReads~TotalReads+0,maxit=1000)
f=rlmfit$coefficients["TotalReads"]
```

Therefore, the estimated fetal fraction (f) for the sample is 0.244.

Maternal-Fetal Genotype Estimation for Polymorphic Sites

For each sample, fetal fraction was estimated using a panel of allelic read counts. Then the genotype for each polymorphic site was estimated using the minimal AIC value as detailed below. First, observed allelic read counts (O_i), total read count (TotalReads) and expected allelic read counts (E_i) for each possible genotype model were calculated for each polymorphic site (O_i is set to 0.1 if O_i = 0 and E_i is set to TotalReads×α if the expected E_i = 0), and then AIC was calculated for each genotype model using the following formula:

$$AIC = 2 \times \sum \left[O_i \times ln\left(\frac{O_i}{E_i}\right)\right] - 2 \times df$$

Where df is the residual degrees of freedom. Finally, the genotype for the polymorphic site was estimated to be the one with the minimal AIC, and AIC difference (ΔAIC) was the absolute difference between the minimal AIC and the second minimal AIC. The adjusted AIC = AIC/f/TotalReads, and the adjusted ΔAIC = ΔAIC/f/TotalReads. AIC could also be calculated using a modified formula as described below and identical genotype estimations were observed for our simulated samples. If only one allele was observed informative, then for model AA|AA, only O_1 and E_1 was used for AIC calculation; for models AB|AA, AB|AB and AA|AB, O_1-O_2 and E_1-E_2 were used; and for model AB|AC, both O_1-O_3 and E_1-E_3 were used. Similarly, if two or three alleles were observed informative, then two or three O_i and E_i were used for AIC calculation depending on the specific fitted genotype model.

For example, the estimated fetal fraction for the imaginary sample is f=0.244 and if the expected model fitting background (α) is set to 0.005, then the observed and the expected allelic read counts were calculated as follows:

For ID-01, observed allelic read counts are [14127, 35, 0], then O_1=14127, O_2=35 and O_3=0.1, TotalReads=R1+R2+R3=14127+35+0=14162, df=3-1=2, f=0.244.

Fitting AA|AA model:
$E_1 = TotalReads \times (1 - 2 \times \alpha) = 14162 \times (1 - 2 \times 0.005) = 14020.38$
$E_2 = TotalReads \times \alpha = 70.81$
$E_3 = TotalReads \times \alpha = 70.81$
$AIC_{AA|AA} = 2 \times \left(O_1 \times ln\frac{O_1}{E_1} + O_2 \times ln\frac{O_2}{E_2} + O_3 \times ln\frac{O_3}{E_3}\right) - 2 \times df = 159.41$
Adjusted $AIC_{AA|AA} = AIC_{AA|AA}/f/TotalReads = 0.046$

Fitting AA|AB model:
$E_1 = TotalReads \times (1 - \alpha) \times (2 - f)/2 = 12372.06$
$E_2 = TotalReads \times (1 - \alpha) \times f/2 = 1719.13$
$E_3 = TotalReads \times \alpha = 70.81$
$AIC_{AA|AB} = 3469.89$
Adjusted $AIC_{AA|AB} = 1.004$

Fitting AB|AA model:
$E_1 = TotalReads \times (1 - \alpha) \times (1 + f)/2 = 8764.78$
$E_2 = TotalReads \times (1 - \alpha) \times (1 - f)/2 = 5326.51$
$E_3 = TotalReads \times \alpha = 70.81$
$AIC_{AB|AA} = 13129.87$
Adjusted $AIC_{AB|AA} = 3.800$

Fitting AB|AB model:
$E_1 = TotalReads \times (1 - \alpha) \times 1/2 = 7045.60$
$E_2 = TotalReads \times (1 - \alpha) \times 1/2 = 7045.60$
$E_3 = TotalReads \times \alpha = 70.81$
$AIC_{AB|AB} = 19279.24$
Adjusted $AIC_{AB|AB} = 5.579$

Fitting AB|AC model:
$E_1 = TotalReads \times 1/2 = 7081.00$
$E_2 = TotalReads \times (1 - f)/2 = 5353.24$
$E_3 = TotalReads \times f/2 = 1727.76$
$AIC_{AB|AB} = 19156.21$
Adjusted $AIC_{AB|AB} = 5.544$

As $AIC_{AA|AA} < AIC_{AA|AB} < AIC_{AB|AA} < AIC_{AB|AC} < AIC_{AB|AB}$, the estimated genotype for ID-01 site is AA|AA.
Minimal AIC=$AIC_{AA|AA} = 159.41$
Minimal adjusted AIC=$Adjusted\ AIC_{AA|AA} = 0.046$
$\Delta AIC = AIC_{AA|AB} - AIC_{AA|AA} = 3469.89 - 159.41 = 3310.48$
Adjusted $\Delta AIC = \Delta AIC/f/TotalReads$
$= Adjusted\ AIC_{AA|AB} - Adjusted\ AIC_{AA|AA} = 1.004 - 0.046 = 0.958$

The AICs for all other sites are calculated similarly and listed below.

Marker ID	Total Reads	AIC					Estimated Genotype	Minimal AIC	Minimal Adjusted AIC
		AA|AA	AA|AB	AB|AA	AB|AB	AB|AC			
ID-01	14162	159.41	3469.89	13129.87	19279.24	19156.21	AA|AA	159.41	0.046
ID-02	4695	2655.61	1.67	1526.69	2996.40	3189.20	AA|AB	1.67	0.001
ID-03	6303	24207.47	5213.19	369.79	9.62	1336.75	AB|AB	9.62	0.006
ID-04	9388	25240.70	4035.06	6.14	555.64	2276.37	AB|AA	6.14	0.003
ID-05	8046	27177.07	8863.34	4777.25	4833.02	-3.01	AB|AC	-3.01	-0.001

Maternal-Fetal Genotype Estimation for Short Genetic Variations

For each site, the maternal-fetal genotype group (AA|AA, AA|AB, AB|AA, AB|AB or AB|AC) was estimated first using its allelic read counts. Then, the wildtype sequence was compared with its different alleles (Table S7, S8) and the maternal-fetal mutational status was determined accordingly. For example, if the target site had the genotype AA|AA, and the R1 allele's sequence was wildtype, then the maternal-fetal genotype was WW|WW, while if the R1's sequence was mutant, then it was MM|MM, where W for wildtype and M for mutant. The wildtype/mutant status for other genotypes could be processed similarly.

Maternal-Fetal Chromosomal/Subchromosomal Abnormality Detection

If a polymorphic site is from a diploid mother carrying a diploid fetus (herein labeled as disomy-disomy for each chromosome), it can only be one of the following five maternal-fetal genotypes, namely AA|AA, AA|AB, AB|AA, AB|AB and AB|AC. However, if the polymorphic site is on the target chromosome of a diploid mother carrying a trisomy fetus (labeled as disomy-trisomy for the target chromosome), it can only be one of the following ten genotypes (AA|AAA, AA|AAB, AA|ABB, AA|ABC, AB|AAA, AB|AAB, AB|AAC, AB|ABC, AB|ACC and AB|ACD). In each cfDNA sample containing a possible trisomy fetal chromosome, all polymorphic sites on the target chromosome are either all disomy-disomy or all disomy-trisomy, but not both. Therefore, for each target polymorphic site, the minimal adjusted AIC for each chromosomal model was calculated first, and then the model that shows best overall fit for all polymorphic sites is selected. To detect fetal chromosomal monosomy, each polymorphic site is tested against all possible genotypes for a chromosome that is possible monosomy in fetus, and the model that shows best overall fit for all polymorphic sites is selected. Subchromosomal deletions/duplications could be detected similarly using all possible chromosomal models for the target chromosome.

For example, the following are imaginary representative allelic read counts on a target chromosome for two samples, and each has five polymorphic sites on the target chromosome (R1-R4: allelic read counts in descending order). Suppose that the target chromosome is chromosome 21, and we want to test if any of the two samples are trisomy 21. Background α is set to 0.01.

SampleId	SiteId	Allelic Counts (Descending)			
		R1	R2	R3	R4
S001	Id001	9565	14	4	0
	Id002	5820	652	6	3
	Id003	6718	4465	12	5
	Id004	7838	7656	34	12
	Id005	9465	7552	1898	33
S002	Id001	7021	1574	7	3
	Id002	10588	1185	1164	23
	Id003	3408	2861	23	12
	Id004	9059	6012	1505	34
	Id005	9386	9373	1899	18

Then each polymorphic site is tested against all genotypes of both the disomy-disomy model and the disomy-trisomy model, and the best fit genotypes for the disomy-disomy model and the disomy-trisomy model are listed below.

Overall Goodness-of-fit Test Results for Different Chromosomal Models

SampleId	SiteId	Best Fit Genotype for Each Model							
		Disomy-Disomy Model				Disomy-Trisomy Model			
		Genotype	TC	G	AIC	Genotype	TC	G	AIC
S001	Id001	AA|AA	9565	0	0	AA|AAA	9565	0	0
	Id002	AA|AB	6472	0.039	-1.961	AA|AAB	6472	7.338	5.338
	Id003	AB|AA	11183	0.025	-1.975	AB|AAA	11183	60.564	58.564
	Id004	AB|AB	15494	2.138	0.138	AB|AAB	15494	97.537	95.537
	Id005	AB|AC	18915	0.054	-3.946	AB|AAC	18915	154.291	150.291
S002	Id001	AA|AB	8595	543.745	541.745	AA|ABB	8595	0.099	-1.901
	Id002	AA|AB	12937	3131.2	3129.2	AA|ABC	12937	0.193	-3.807
	Id003	AB|AB	6269	47.789	45.789	AB|AAB	6269	0.084	-1.916
	Id004	AB|AC	16576	143.656	139.656	AB|AAC	16576	0.077	-3.923
	Id005	AB|AC	20658	245.48	241.48	AB|ABC	20658	0.266	-3.734

For the sample S001, nearly all polymorphic sites fit the disomy-disomy model better than the disomy-trisomy model, hence chromosome 21 in the sample S001 is normal for both the mother and the fetus.

For the sample S002, all polymorphic sites fit the disomy-trisomy model better than the disomy-disomy model, hence chromosome 21 in the sample S002 is normal for the mother and trisomy for the fetus.

Plotting Distributions of Relative Allelic Read Counts

For the disomy-disomy model, five maternal-fetal genotypes are possible and there are at most three alleles for each polymorphic site. Hence, knowing the relative allelic counts for any two alleles is informative enough to calculate the relative counts for the third one. Therefore, for each polymorphic site, allelic read counts were calculated and labeled as R1, R2 and R3, whereas

R1≥R2≥R3, and then the relative allelic counts RRC1=R1/(R1+R2+R3) and RRC2= R2/(R1+R2+R3) were calculated, followed by the plotting of RRC2 against RRC1. For the disomy-monosomy model or the subchromosomal deletion model, RRC1 was plotted against RRC2 similarly for each polymorphic site, and distinct clusters corresponding to different chromosomal genotypes were shown in the generated plot. As there were at most four alleles for each polymorphic site for the disomy-trisomy model or the subchromosomal duplication model, RRC1 was calculated as R1/(R1+R2+R3+R4), RRC2 as R2/(R1+R2+R3+R4) , RRC3 as R3/(R1+R2+R3+R4) and RRC4 as R4/(R1+R2+R3+R4) . Then, RRC2 and RRC4 were plotted against RRC1 for the disomy-trisomy model, while RRC2 and RRC3 were plotted against RRC1 for the subchromosomal duplication model to distinguish all possible genotypes graphically.

Plotting Short Genetic Variations

For each polymorphic site, the wildtype allele (R_w) was counted first followed by the count of mutant alleles as R_{m1}, R_{m2}, R_{m3}, whereas $R_{m1}\geq R_{m2}\geq R_{m3}$. Then the relative mutant allele 1's count (R_{m1}/TotalCount) was plotted against the relative wildtype allele count (R_w/TotalCount) and all the possible maternal-fetal wildtype-mutant genotypes could be identified on the generated graph easily.

Fetal Fraction Estimation for cfDNA samples from surrogate mothers

For cfDNA samples from surrogate mothers, at most 4 alleles are possible for each polymorphic site on a normal chromosome. To estimate fetal fraction using a panel of polymorphic sites (Fig. S15), an initial fetal fraction estimate (f_0) is set, followed by iteratively updating f_0 until converge. To update f_0, allelic goodness-of-fit test is performed for each polymorphic site to select the best fit genotype under the current f_0 estimate, followed by the estimation of read count derived from fetal genetic materials (FC, FetalReads) and the total read count (TC, TotalReads) , and then new fetal fraction (f) is estimated by fitting a rlm model using the FCs and TCs of all polymorphic sites. Finally f_0 is set to f, f_0 is updated iteratively until the change of f_0 for each iteration is very small ($|f-f_0|<\varepsilon$).

For example, the following are imaginary representative allelic read counts for nine polymorphic sites from a sample (R1-R5: allelic read counts in descending order). Background α is set to 0.01, ε=0.001.

SiteId	Allelic Counts				
	1	2	3	4	5
Id001	35	14127			
Id002	4105	577	13	7	9
Id003	54	3101	3148	23	
Id004	11	5809	27	3552	17
Id005	3028	1011	4007	6	6
Id006	36	936	3322	28	16
Id007	5422	52	974	938	27
Id008	1498	4835	1537	4711	38
Id009	36	3412	2237	3493	23

Step 1, set f_0=0.10 (initial estimate).

Step 2, for each polymorphic site, estimate FC and TC using allelic goodness-of-fit test. For example, for site Id006, R1 to R4 are set to 3322, 936, 36 and 28. As R2/(R1+R2)≥α and R3/(R1+R2+R3)<α, there are two informative alleles. The allelic counts R1 to R4 are tested against 9 genotype models (AA|AA, AA|AB, AB|AA, AB|AB, AB|AC, AA|BB, AA|BC, AB|CC, AB|CD) assuming fetal fraction is f_0. As the best fit genotype for Id006 is AA|BB, FC=936 and TC=4258. FCs and TCs for all other polymorphic sites are estimated similarly.

Step 3, calculate fetal fraction f by fitting a robust linear regression model for all FC and TC pairs.

Step 4, if $|f-f_0|>\varepsilon$, then set f_0=f and execute Step 2; else the fetal fraction is estimated as f.

The iterative results for the above example are listed below.

Iterative Results for Fetal Fraction Estimation

Iterative Step	f_0	f	$\|f-f_0\|$
1	0.1	0.2385	0.1385
2	0.2385	0.2436	0.0051
3	0.2436	0.2436	0

Therefore, the estimated fetal fraction (f) for the sample is 0.2436.